70-20,010

BRUSTKERN, Richard Lee, 1931-
AN ANALYTICAL TREATMENT OF TWO-PHASE FLOW DURING INFILTRATION.

Colorado State University, Ph.D., 1970
Engineering, civil

University Microfilms, A XEROX Company, Ann Arbor, Michigan

DISSERTATION

AN ANALYTICAL TREATMENT OF TWO-PHASE FLOW DURING INFILTRATION

Submitted by
Richard Lee Brustkern

In partial fulfillment of the requirements
for the Degree of Doctor of Philosophy
Colorado State University
Fort Collins, Colorado
March 1970

COLORADO STATE UNIVERSITY

March 1970

WE HEREBY RECOMMEND THAT THE DISSERTATION PREPARED UNDER

OUR SUPERVISION BY Richard Lee Brustkern

ENTITLED An Analytical Treatment of Two-Phase Flow During Infiltration

BE ACCEPTED AS FULFILLING THIS PART OF THE REQUIREMENTS FOR THE DEGREE OF DOCTOR OF PHILOSOPHY

Committee on Graduate Work

Norman A. Evans

Major Professor

Melvin E. Holland

J W Fead

J W Fead

Head of Department

Examination Satisfactory

Committee on Final Examination

Melvin E. Holland

J W Fead

Norman A. Evans

Chairman

Permission to publish this dissertation or any part of it must by obtained from the Dean of Graduate School.

ABSTRACT

The problem of one-dimensional infiltration into a homogeneous porous medium is given an approximate analytical treatment. Movement of both the air phase and the water phase is considered.

The treatment is made possible by assuming that capillary pressure can be partially neglected. When the continuity equation, and Darcy's law for each phase are combined with the assumption that capillary pressure can be neglected, an equation involving saturation displacement and an average total velocity, as the unknowns, is obtained. A second equation, involving these two unknowns, is obtained by combining the capillary pressure relationship, and Darcy's law for each phase, and then integrating at a fixed time t. These two relationships are solved in a step-wise manner to yield the saturation profile, and then the infiltration rate, at time t. Soil properties and relationships which are required for the analysis are porosity, intrinsic permeability, relative permeability versus saturation relationships, and the capillary pressure versus saturation relationship.

Infiltration rate curves are obtained for a number of situations involving different boundary and/or initial conditions. Comparisions are made with experimental results, as well as with results obtained from a finite difference solution.

Richard Lee Brustkern
Department of Civil Engineering
Colorado State University
Fort Collins, Colorado
March 1970

ACKNOWLEDGMENTS

The author wishes to recognize the contributions made to this dissertation by his major professor and advisor, Dr. Hubert J. Morel-Seytoux, Associate Professor of Civil Engineering. Frequent discussions with Dr. Morel-Seytoux provided valuable assistance in the analysis of the problem.

Appreciation is also extended to the other members of the committee on graduate study; Dr. J. W. N. Fead, Professor and Head of the Civil Engineering Department; Dr. N. A. Evans, Director of the Natural Resources Center; and Dr. M. E. Holland, Assistant Professor of Civil Engineering.

The writer also wishes to acknowledge the Financial assistance provided for this study by the Office of Water Resources Research of the United States Department of Interior, as authorized under the Water Resources Research Act of 1964 (Public Law 88-379).

TABLE OF CONTENTS

LIST OF FIGURES

LIST OF FIGURES - Continued

LIST OF FIGURES - Continued

LIST OF SYMBOLS

Symbol	Definition	Dimensions
D	Water table depth	L
f_a	Fractional flow function form for air when gravity and capillary pressure are neglected	
FW	Fractional flow function for water (V_w/V)	
F_w	Fractional flow function form when capillary pressure is neglected	
F'_w	$\frac{dF_w}{dS_w}$	
f_w	Fractional flow function form when gravity and capillary pressure are neglected	
f'_w	$\frac{df_w}{dS_w}$	
g	Acceleration of gravity	L/T^2
H	Depth of water ponding at the surface	L
k	Intrinsic permeability of soil	L^2
k_{ra}	Relative permeability of soil to air	
k_{rw}	Relative permeability of soil to water	
p_A	Atmospheric pressure	M/LT^2
p_a	Pressure in the air phase	M/LT^2
p_c	Capillary pressure (p_a-p_w)	M/LT^2
p_w	Pressure in the water phase	M/LT^2
QT	Average infiltration rate per unit area during a given time interval	L/T
S_{ar}	Residual saturation of air	
S_w	Saturation of water	
S_{wi}	Initial saturation of water	
S_{wr}	Residual saturation of water	
t	Time	T

LIST OF SYMBOLS (continued)

Symbol	Definition	Dimensions
v	Volume	L^3
V	Average total velocity $(V_w + V_a)$	L/T
V_a	Average velocity of air in the two-phase flow region	L/T
V_w	Average velocity of water in the two-phase flow region	L/T
WT	Quantity of water infiltrated during a given time interval	L^3
z	Vertical cordinate (positive in the downward direction)	L
z_{S_w}	Displacement of a particular saturation	L
λ_a	$\frac{k\ k_{ra}}{\mu_a}$	L^3T/M
λ_w	$\frac{k\ k_{rw}}{\mu_w}$	L^3T/M
μ_a	Viscosity of air	M/LT
μ_w	Viscosity of water	M/LT
ρ_a	Density of air	M/L^3
ρ_w	Density of water	M/L^3
$\Delta\rho$	Density difference $(\rho_w - \rho_a)$	M/L^3
ϕ	Porosity of soil	

Chapter 1

INTRODUCTION

For the purposes of this study infiltration will be defined as the movement of water from the surface of the ground into the soil.

Infiltration influences the amount of runoff which results from a given rainfall; it replenishes the groundwater supply; it provides water for nearly all forms of plant life. The infiltration process is therefore not only of hydrologic importance but also of considerable economic importance.

From a hydrologic point of view, it would be desirable to be able to predict the response of a watershed to a particular rainfall event, and since infiltration is an important factor in the hydrologic response of a watershed, it is apparent that an ability to predict infiltration rates and quantities is needed. It is toward this need that this study is directed.

The process of infiltration into a soil is an unsaturated flow phenomenon. The flow involves two essentially immiscible fluids: air and water. When water enters a soil, air is replaced; and when water is removed, air must re-enter. It should be pointed out that although this discussion is confined to an air-water system, the theory would be applicable to any system of two immiscible fluids.

The vertical, unsteady flow of water and air in a porous medium may be described by a second order, nonlinear, partial differential equation for water saturation. This equation may be arrived at by combining the principle of continuity, or conservation of mass, Darcy's law for each phase, and the capillary pressure relationship. The derivation is presented in Appendix 1. The resulting differential equation may be written as

$$\phi \frac{\partial S_w}{\partial t} = - \frac{\partial}{\partial z} \left\{ VF_w + \frac{k \; k_{ra}\left(S_w\right)}{\mu_a} f_w \frac{dp_c}{dS_w} \frac{\partial S_w}{\partial z} \right\} \qquad (1)$$

where ϕ is porosity, S_w is water saturation, V is the total velocity, F_w, a form of the fractional flow function as developed in Appendix 1, is equal to the ratio of the water velocity to the total velocity, k is the intrinsic permeability, k_{ra} is the relative permeability of air, μ_a is the viscosity of air, f_w is the fractional flow function with the effects of both capillary pressure and gravity neglected, p_c is the capillary pressure, t is time, and z is the vertical coordinate (positive downward).

This equation is often called the saturation equation and, in this and various other forms, has been the basis for much of the work to date in partially saturated media.

Equation (1) is second order in the independent variable z and first order in the independent variable t. This indicates that two boundary conditions and one initial condition must be specified to insure a unique solution. The functional relationships between k_{ra} and

S_w, between k_{rw} and S_w, and between p_c and S_w must also be defined before a solution can be obtained.

The saturation equation is a mathematical representation of the physical phenomenon of flow in unsaturated porous media. However the complexity of the mathematical expression makes an analytic solution extremely difficult if not impossible. As a result, most researchers have done one of two things: make certain simplifying assumptions in order to reduce the mathematical complexity of the problem, and/or attack the problem utilizing numerical techniques.

It is proposed in this study that certain simplifying assumptions be made. The key assumption to be made is that the capillary pressure can be neglected in the saturation equation — a technique which has been used extensively in the petroleum industry. When the capillary pressure is neglected, Buckley and Leverett (1) have demonstrated that the velocity with which a particular saturation value moves is given by an expression of the following form:

$$\left(\frac{dz}{dt}\right)_{S_w} = \frac{V}{\phi}\frac{dF_w}{dS_w} = \frac{V}{\phi}F'_w \qquad (2)$$

The details of the development of this equation are presented in Appendix 1.

Now if all of the characteristics of the medium are considered to be constant, equation (2) can be integrated to give the position of a particular saturation value as a function of time:

$$z_{S_w} = z_o + \frac{V}{\phi} F'_w t \tag{3}$$

where z_o is the position of the particular saturation value at time t_o. If V were known, equation (3) would provide a means for determining the saturation profile at any time t, that is, simply compute z_{S_w} for various values of S_w at time t.

In the infiltration problem, V will generally vary with time and will not be known. However it is possible to develop an integral equation relating V to the pressures at two positions: immediately ahead of the advancing moisture front and immediately below the ground surface (Appendix 1). Thus, computation of these two pressures provides a means of determining V at a given time. The equation, which relates these quantities, is

$$-\int_1^2 dp_w + \int_1^2 \rho_w g dz = V\int_1^2 \frac{dz}{k\left(\frac{k_{ra}}{\mu_a} + \frac{k_{rw}}{\mu_w}\right)} + g(\rho_w - \rho_a)\int_1^2 (1-f_w) dz + \int_1^2 (1-f_w) dp_c \tag{4}$$

Equations (3) and (4) then provide the basic tools to be used in this investigation. With these tools it will be possible to determine the saturation profile at any time t. Once the saturation profile is known at time t, the quantity of infiltration, which has occurred up to time t, can be computed by integration and the infiltration rate can be determined by differentiation. The details concerning the application of this technique are presented later in this paper. The method will be applied to several problems with different boundary conditions.

It should be emphasized that the approach presented in this paper does consider the movement of the air phase, as well as the movement of the water phase. The influence of air compressibility on the flow phenomenon is also considered. These are two aspects of unsaturated flow which have been generally neglected in previous studies.

It should also be noted that although capillary pressure effects were neglected in arriving at equation (3), no such assumption was made in the development of equation (4). Therefore the capillary effects are not neglected entirely in determining the saturation profile. They will be felt to some degree through the term V in equation (3).

It has previously been pointed out that unless the saturation equation is to be treated by some numerical scheme, it is necessary to make certain simplifying assumptions in order to make the problem mathematically tractable. The partial neglect of capillary pressure reduces the complexity of the problem and results in simplified computational procedures, and if meaningful estimates of infiltration quantities can be obtained with the simplified computational procedures, there is some justification for neglecting capillarity. In addition, it is thought that capillary pressure effects are felt primarily in a relatively narrow zone behind the advancing saturation front. For it is in this region that the saturation gradient $\frac{\partial S_w}{\partial z}$, which appears in equation (1), is steep. This means that although the capillary pressure may be important in determining the shape of the saturation profile, it is probably of a much lesser importance in determining the quantity of water infiltrated. And as the profile lengthens with time, the effect of capillary pressure on infiltration quantities should diminish further. Since the primary purpose of this investigation is to determine infiltration quantities rather than saturation profiles "per se", the seriousness of partially neglecting capillarity effects is lessened.

Chapter II

LITERATURE REVIEW

The process of infiltration involves the flow of fluids through a porous medium. Theory and application practices pertaining to porous-media flow have originated in fields such as oil production, hydraulics, soil mechanics, chemical engineering, soil science, hydrology, agricultural engineering, and others. Periodicals concerned with these fields provide a comprehensive coverage of the past and present endeavors in the general area of porous-media flow.

Buckingham (2) is usually credited with being the first to propose explicitly that the rate of water movement in an unsaturated soil might be proportional to the gradient of the capillary potential. In his notation,

$$Q = \lambda \frac{\partial \psi}{\partial x}$$

where Q is the flux of water per unit area, λ is the capillary conductivity, and ψ is the capillary potential. Buckingham also expressed the equation in terms of the water content gradient:

$$Q = \lambda \frac{\partial \psi}{\partial \theta} \frac{\partial \theta}{\partial x}$$

which implies that a relationship exists between water content θ and the capillary potential. The water content is the fraction of the bulk volume occupied by water.

In a 1911 paper, Green and Ampt (3) presented several equations describing the movement of water in soils. These equations were based on a capillary tube model of flow in porous media. Implicit in the use of a capilllary tube model is the assumption that all the pores behind the wetting front are filled with water. Green and Ampt realized that this was not the case during infiltration into a porous medium but considered the assumption to be a reasonable approximation.

Buckingham's equation was combined with the continuity equation by Gardner and Widstoe (4) in 1921. The resulting partial differential equation was solved by assuming an empirical relationship between capillary potential and soil water content. They also assumed a constant capillary conductivity. From these assumptions they derived an infiltration equation of the form

$$f_t = f_\infty + (f_\circ - f_\infty)e^{-\beta t}$$

where f_t is the infiltration rate at time t, $f_\circ$ is the infiltration rate when $t=0$, f_∞ is the final infiltration rate, and β is a soil parameter.

Although there were exceptions, some of which are noted above, the infiltration process was generally given a rather limited and qualitative treatment through the 1920s. Then in the early 1930s an increased interest in the process developed. This increased interest was directed primarily toward two different approaches. One approach was to develop empirical infiltration relationships based primarily on experimental results. The other approach was to work with the basic differential equation which described the phenomenon of flow through a porous medium.

The empirical relationships typically indicate infiltration rates to be a function of time, dependent on the initial soil moisture content and the physical properties of the soil. The experimental evidence, on which the equations were based, was usually obtained from infiltrometer data or an analysis of runoff hydrographs along with the rainfall patterns which produced them.

One of the early empirical relationships was suggested by Kostiakov (5) in 1932. His equation describes the relationship between the cummulative infiltration and time in a power relation of the form:

$$F = kt^{\alpha}$$

where k and α are parameters of the soil. The infiltration rate, which may be obtained by differentiation, is

$$I = k\alpha t^{\alpha-1}$$

Additional empirical relationships, which vary in form, have been proposed by other investigators through the years. Among the more well known relationships is that presented by Horton (6) in a 1940 paper. Horton proposed an empirical equation similar to that of Gardner and Widstoe, except that his interpretation of β was slightly different. His equation is

$$f = f_c + (f_o - f_c)e^{-\beta t}$$

where f_c is the final constant rate of infiltration, f_o is the initial infiltration rate, and β is a parameter depending on the soil and vegetation. The quantities f_o, f_c, and β must be known if this equation is to yield meaningful infiltration rates. The quantity f_c is usually well defined for a given soil-vegetation complex. However f_o is not so well defined and experimental evidence shows that f_o changes with antecedent moisture conditions. It is higher for initially dry conditions and decreases with increasing initial moisture content. The rate of recession of the infiltration rate is influenced by β, and β is usually assumed to be constant for a given soil-moisture complex.

One other relationship, which was proposed by Holtan (7), will be mentioned. Holtan suggests that the infiltration versus time relationship could be obtained by considering some potential volume of infiltration F_p. F_p represents the volume which is still available for infiltration above some arbitrary depth. The rate of infiltration is considered to be a function of this potential volume at any time before the final constant infiltration rate f_c is reached. Holtan's relationship is

$$f - f_c = aF_p^{\,n}$$

where a and n are constant for a given soil complex. The primary difficulty in applying this equation lies in the determination of the parameters involved.

A general criticism, which can be leveled against most of the empirical relationships, is that it is possible to attach only a gross kind of physical significance to many of the parameters in the various equations.

At about the same time that Kostiakov proposed his empirical equation for infiltration, Richards and others were attempting to better understand and quantify the movement of water in saturated and unsaturated porous media. The approach taken by these investigators was based on a mathematical representation of the physical phenomenon involved. Physically, it is a much more acceptable approach than the empirical approach.

When Darcy's law for each phase, the continuity equation for each phase, and the capillary pressure relationship are combined, the result is a general equation which describes the flow in a porous medium. This equation is commonly called the saturation, flow, or soil moisture equation and may be written in a variety of forms. Equation (1) of this paper is one form for the case of one-dimensional, vertical flow. The mathematics of the saturation equation have proved to be extremely complex. The measurement of physical parameters for use in the mathematical relationship has also presented a formidable obstacle. As previously stated, these difficulties have generally caused investigators to follow one of two procedures: reduce the mathematical complexity of the problem by making simplifying assumptions and/or attack the problem using numerical techniques.

In 1931 Richards (8) combined Darcy's law and the continuity equation for the water phase only and obtained an equation similar to that of Gardner and Widstoe:

$$\frac{\partial \theta}{\partial t} = \frac{\partial}{\partial x} K \frac{\partial \psi}{\partial z} - \frac{\partial K}{\partial x}$$

where θ is the water content, K is the capillary conductivity, and ψ is the capillary potential. Implicit in this type of equation is the assumption that the resistance due to the flow of air is negligible.

An equation of the diffusion type was proposed by Childs (9). He reasoned that since K and ψ were both functions of the water content, Richard's equation could be written in the simpler form

$$\frac{\partial \theta}{\partial t} = \frac{\partial}{\partial x}(D\frac{\partial \theta}{\partial \chi}) - \frac{\partial K}{\partial x}$$

where $D = K \frac{d\psi}{d\theta}$ is the diffusivity. Childs first studied the problem assuming a constant diffusivity. Then in a later paper by Childs and Collis-George (10), the more realistic concentration dependent diffusivity was introduced.

In 1952 Klute (11) adopted a numerical solution from Crank and Henry (12) to solve the diffusion equation with concentration dependent diffusivity for the horizontal flow problem.

Philip treated the problem of infiltration in some detail in a series of papers (13, 14, 15, 16, 17). With a procedure that is basically analytic (although some numerical methods are required), Philip arrived at a solution for the horizontal flow problem. He later extended his solution to the vertical infiltration problem by following a sequence of approximations. Philip found that when water was applied at a constant rate to a semi-infinite medium, whose initial moisture content was uniform, the total infiltration was given by an expression of the form

$$i = St^{\frac{1}{2}}, + At + Bt^{\frac{3}{2}} + - - -$$

where t is time and $S, A, B, - - -$ are functions of the water content and must be solved for numerically. The author reported that the series converges rapidly for the infiltration problem and that only the first few terms need be evaluated. As t becomes large, the above equation becomes unreliable. Philip proposed another method suitable for large t.

A weakness in the approach of Philip and the others who worked with the diffusion-type equation is the neglect of resistance to the flow of air. This resistance might be expected to be appreciable in situations where the air is not free to escape.

Recent advances in computer technology have resulted in increased efforts toward numerical solutions of the saturation equation. The general procedure is to substitute difference approximations for the corresponding derivatives in the saturation equation. The resulting relationships are applied to the nodes of a net which covers the solution domain. A variety of finite difference approximations (forward, backward, or central difference forms) may be used in solving the resulting equations to obtain an approximate solution.

A large number of investigators have utilized numerical methods to attack the saturation equation. A variety of boundary conditions, initial conditions, and numerical schemes have been applied to the various forms of the saturation equation. Among others, Hanks and Bowers (18), Rubin and Steinhardt (19), Whisler and Klute (20), and Ibrahim (21) have been active in this area. Freeze (22) presents a good summary of the work which has been done in the field.

Numerical methods permit the treatment of a variety of infiltration problems with a minimum of simplifying assumptions required. However, the procedures require large-capacity computers and are quite costly. In addition, the methods provide little insight into the physical processes involved.

Concurrent with the previously mentioned advances in the fields of soil science and hydrology were similar advances in the petroleum industry. Although these developments were not associated with the infiltration problem directly, they do provide a further understanding of the general problem of porous-media flow. One development, in particular, will be used extensively in the treatment of the infiltration problem in this paper. That development is the work of Buckley and Leverett.

In 1942 Buckley and Leverett (1) introduced a concept in displacement theory which has proved very useful in the oil industry. The details of the development are presented elsewhere in this paper. Basically though, Buckley and Leverett's approach was to neglect capillary pressure and air compressibility and consider the path of a given saturation value. That is, they determined at what time t a given saturation value would be at a particular position x. For horizontal flow their relationship takes the form

$$x_{S_w} = \frac{V}{\phi} f'_w t + x_o$$

where x_{S_w} is the position of the water saturation at time t, x_o is the position of the water saturation at time t_o, V is the total velocity, ϕ is the porosity, t is the time, and f'_w is the derivative of the fractional flow function with respect to saturation.

This equation provides a means of constructing the saturation profile at any time t. However, as time progresses, the saturation becomes a multiple valued function of the distance coordinate x. Buckley and Leverett interpreted the formation of multiple values as an indication that the saturation distance curve had become discontinuous. They devised a method for determining the position of the discontinuity (front) from a material balance.

A 1952 paper by Welge (23) provides a graphical means of determining the Buckley-Leverett front under certain circumstances. The technique is not applicable during certain transition stages. However when applicable, the technique eliminates the need for a material balance to determine the position of the front. The material balance is actually guaranteed by the graphical construction.

Martin (24) deals with the application of the Buckley-Leverett method to a variety of problems. Although the problems are from the petroleum industry, they do provide an understanding of the utility of the method. An unpublished report by Morel-Seytoux (25) for the Chevron Research Company also provides some excellent examples of the applicability of the Buckley-Leverett scheme.

The combined method of Buckley, Leverett and Welge greatly simplifies the problem of displacement of one immiscible fluid by another. The graphical techniques which are utilized are quite useful in visualizing the movement of the moisture into the porous medium. The main criticism, of course, has to do with the validity of neglecting capillary pressure. Although this neglect is justified under certain circumstances, it may not be under other circumstances. This limitation is treated in more detail elsewhere in this paper.

Each of the investigations discussed in this chapter represents a contribution to the general understanding of the infiltration process and, as such, is important to the concepts developed in the remainder of this paper. However, as previously indicated, the ideas of Buckley and Leverett provide the real basis for the developments in the remaining chapters.

Chapter III

ANALYTICAL CONCEPTS AND PROCEDURES

The objective of this study is to develop a new and practical technique for determining infiltration rates. In order to achieve this objective, certain basic concepts must be employed. It is the purpose of this chapter to qualitatively discuss these concepts along with the associated computational procedures.

At any time t the quantity of water which has infiltrated is proportional to the area under the corresponding saturation profile (S_w vs z). Thus the construction of the saturation profile is a necessary preliminary step to a determination of infiltration quantities. It has previously been stated that equations (3) and (4) provide a means of constructing the saturation profile at any time t. As indicated in the introductory chapter, saturation displacements may be determined by equation (3),

$$z_{S_w} = z_o + \frac{V}{\phi} F'_w t \tag{3}$$

and the total velocity may be determined by equation (4),

$$-\int_1^2 dp_w + \int_1^2 \rho_w g dz = V \int_1^2 \frac{dz}{k\left(\frac{k_{ra}}{\mu_a} + \frac{k_{rw}}{\mu_w}\right)} + g(\rho_w - \rho_a)\int_1^2 (1-f_w) dz + \int_1^2 (1-f_w) dp_c \tag{4}$$

Examination of equation (3) reveals that the saturation profile, specifically z_{S_w}, depends upon the total velocity V. Similarly, equation (4) indicates a dependence of V upon z. This suggests the simultaneous solution of this system of two equations. However, the computational difficulties can be reduced and at the same time a good approximate solution obtained if the equations are instead solved in the following step-wise manner. A very slightly extended initial saturation profile will be assumed to exist at t_o. From this assumed profile and the known boundary conditions, a total velocity V will be computed using equation (4). This newly computed V will be considered to represent the total velocity from time t_o to $t_o + \Delta t$ and will be used in equation (3) to calculate a new saturation profile at $t_o + \Delta t$. The quantity of water infiltrated during Δt is proportional to the change in the area under the saturation profile and is given by

$$WT = \phi \int S_w dz \Big|_{t = t_o + \Delta t} - \phi \int S_w dz \Big|_{t = t_o} \tag{5}$$

The average infiltration rate during Δt then is

$$QT = \frac{WT}{\Delta t} \tag{6}$$

Based always on the most recently computed profile, this same procedure can be repeated at each succeeding time step.

The accuracy of this approximate solution depends upon how rapidly the total velocity V changes with time.

Experiments show that during the early stages of infiltration V decreases rapidly from an initially high value. Then, as time goes on, V levels off and approaches a constant value. Thus it will be necessary to begin with short time increments which may then be lengthened as the infiltration process proceeds.

In equation (3) it can be seen that the displacement of an individual saturation value depends upon F'_w. In equation (4) V is seen to be a function of f_w. Since f_w is a form of the fractional flow function and F'_w is a derivative of a form of the fractional flow function, the question of the nature of the fractional flow function arises.

3.1 The Properties and Behavior of the Fractional Flow Function

The fractional flow function is defined as the ratio of the water velocity to the total velocity. From the development in Appendix 1, a general form of the function may be written as

$$FW = \frac{V_w}{V} = f_w\left[1 + \frac{k\,k_{ra}}{\mu_a\,V}\left(\frac{\partial p_c}{\partial z} + \Delta\rho g\right)\right]$$

where f_w is defined as

$$f_w = \frac{\dfrac{k\,k_{rw}}{\mu_w}}{\dfrac{k\,k_{rw}}{\mu_w} \quad \dfrac{k\,k_{ra}}{\mu_a}} = \frac{1}{1 + \dfrac{k_{ra}}{k_{rw}}\,\dfrac{\mu_w}{\mu_a}}$$

Now if both capillary pressure and gravity effects are neglected in the general equation,

$$FW = f_w = \frac{1}{1 + \frac{k_{ra}}{k_{rw}} \frac{\mu_w}{\mu_a}} \qquad (7)$$

Since k_{ra} and k_{rw} are functions of saturation only, f_w is also a function of saturation only. It is this fact that makes this form of the fractional flow function very useful.

When just capillary effects are neglected in the general equation, the result is

$$FW = F_w = f_w[1 + \frac{k\ k_{ra}}{\mu_a V} \Delta\rho g] \qquad (8)$$

Only when the quantity $\frac{k}{V}$ is constant does F_w depend on saturation alone and therefore retain its usefulness. However this quantity will normally vary because the properties of the reservoir vary in space and/or because the conditions that induce fluid flow vary in both time and space. But the total velocity V has previously been assumed to be constant over a given time increment. If it is further assumed that the medium is homogeneous, then for a given time increment and within a given zone F_w will be a function of saturation only. These assumptions will be employed in this study.

The properties and behavior of the functions f_w and F_w can best be illustrated by considering their graphical representation. Since f_w is a function of the relative permeabilities, k_{ra} and k_{rw}, the characteristic form of the f_w vs S_w curve can be deduced from the relative permeability curves. Figure 1 shows two typical curves of relative permeability. In the figure, the quantities S_{ar} and S_{wr} represent the residual saturations of air and water respectively. S_{ar} is the saturation above which air is not mobile and S_{wr} is the saturation below which water is not mobile. It is apparent from the form of the curves in Fig. 1 and the functional relationship for f_w, that the f_w vs S_w curve must take on a characteristic S-shape as shown in Fig. 2.

When the effects of gravity are included,as is appropriate in the infiltration problem, the fractional flow relationship is given by equation (8). An examination of this equation suggests that F_w may become greater than 1 at the upper end of the saturation range if $\frac{k\,k_{ra}}{\mu_a V}\Delta\rho g$ is positive and large. Similarly, if $\frac{k\,k_{ra}}{\mu_a V}\Delta\rho g$ is negative, F_w may become negative at the lower end of the saturation range. However, the only way in which $\frac{k\,k_{ra}}{\mu_a V}\Delta\rho g$ may be negative is if $V = V_a + V_w$ is negative. In the chosen coordinate system velocity is positive in the downward direction, and since capillary effects are to be neglected, there is no force present to cause the water in the unsaturated zone to move upward. Therefore V_w may

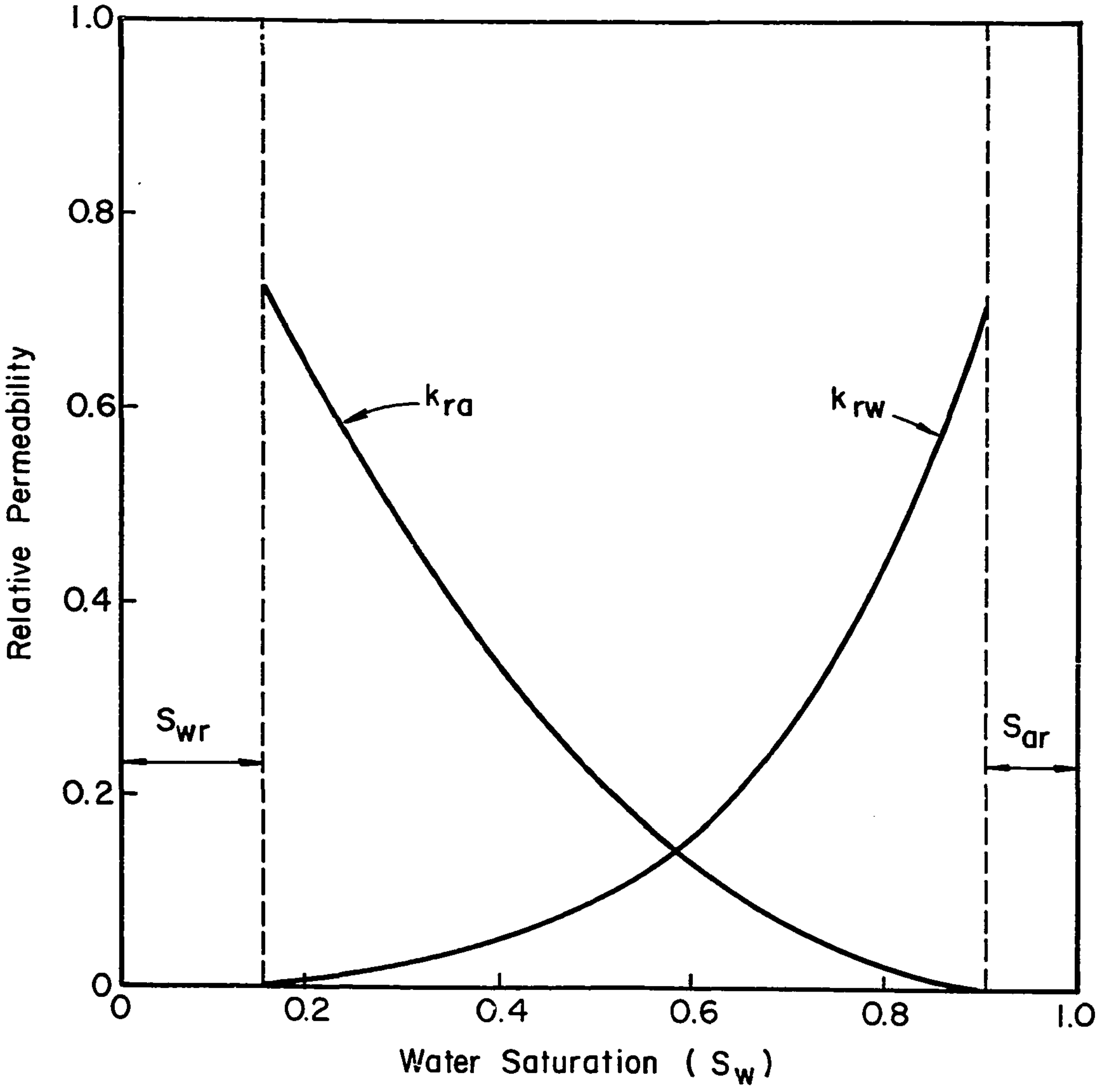

Figure 1 Typical Curves of Relative Permeability

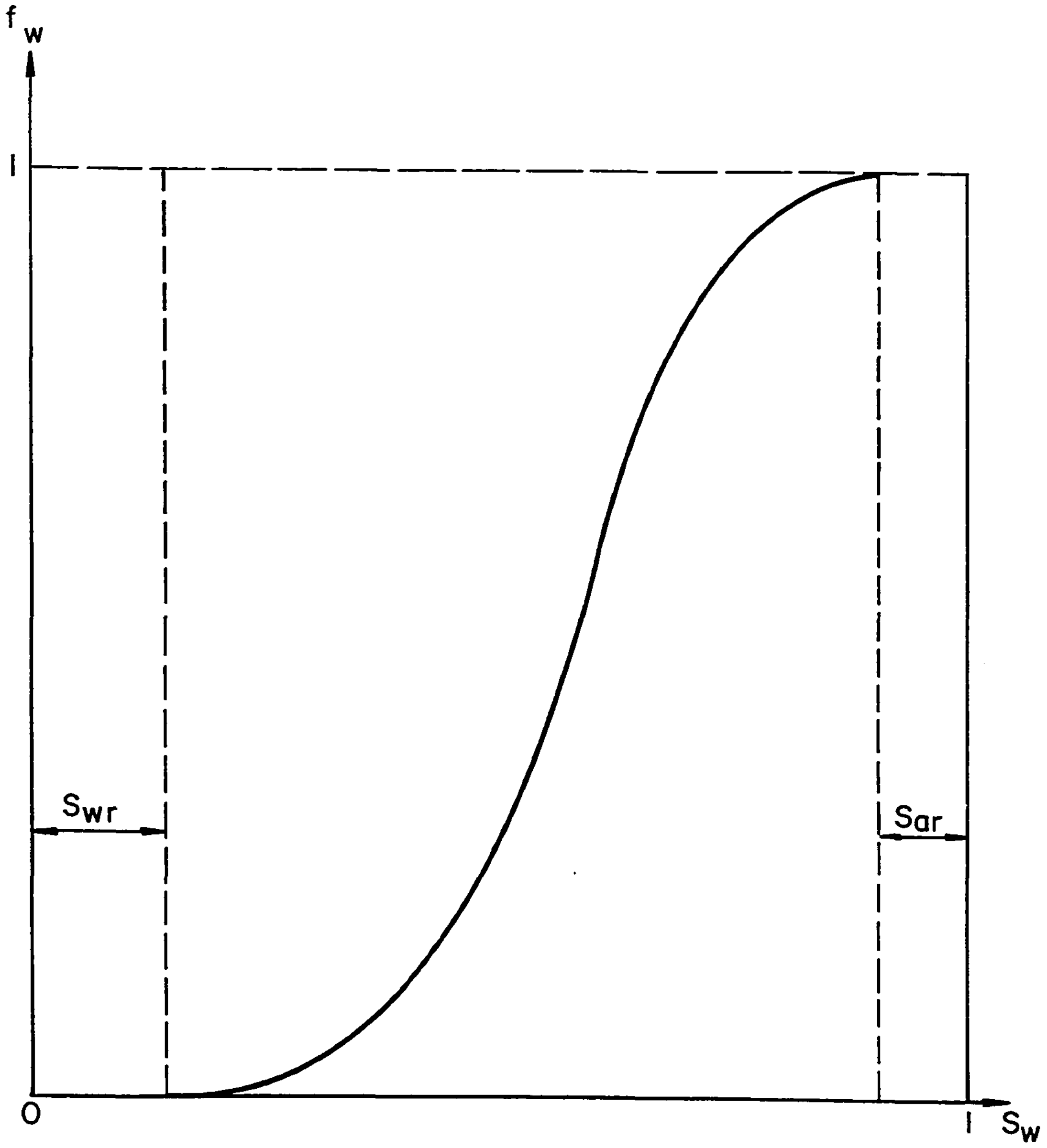

Figure 2 Typical Fractional Flow Function Curve

not be negative. But what about V_a? The air moves as a result of being driven out of the pore space by the water. Thus, although V_a may be negative, the absolute value of its magnitude can not exceed the magnitude of V_w. Therefore it can be concluded that

$$V = V_a + V_w \geq 0$$

and as a result, F_w can not become negative. Consequently when capillarity is neglected in the infiltration problem, the fractional flow function may take forms similar to those shown in Fig. 3. In this figure F_{w_1} represents an F_w curve for a low value of V and F_{w_2} for a high value of V.

A question arises as to the significance of F_w being greater than 1. From the definition of F_w,

$$F_w = \frac{V_w}{V} = \frac{V_w}{V_w + V_a}$$

it is apparent that a value of F_w greater than 1 implies

$$V_w > V_w + V_a$$

The only way in which V_w could be greater than $V_w + V_a$ is that V_a be negative, that is, the air moves upward. The flow of one fluid in a direction opposite to the total flow is termed counterflow. Thus at a high total velocity (as might be expected during the early stages of infiltration) the value of F_w remains less than 1, and the movement of both the air and the water is downward. Later in

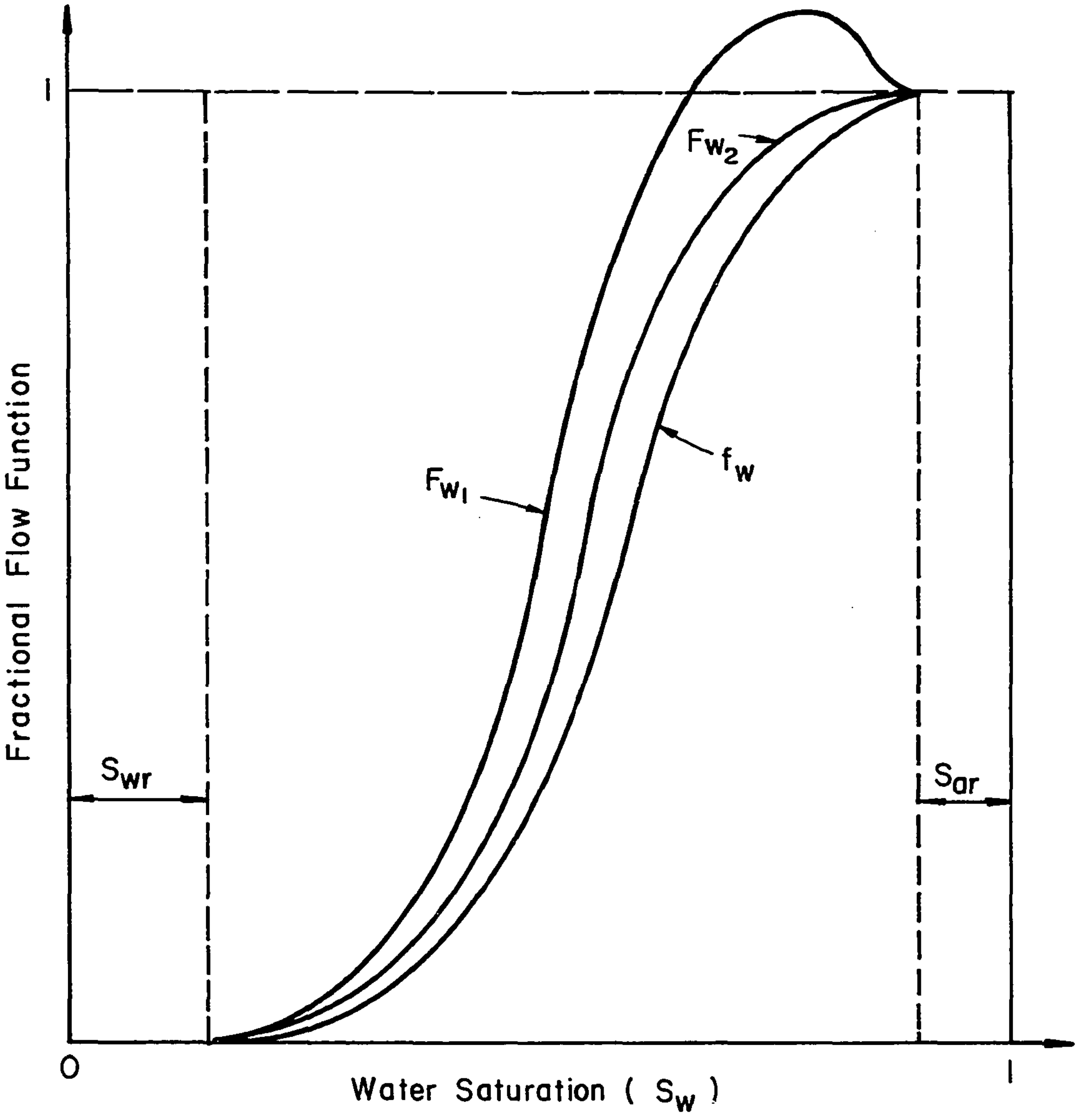

Figure 3 Typical Fractional Flow Function Curves

the infiltration process the value of V decreases and F_w may exceed 1 over some saturation range. If this occurs, a counterflow of air will result within this saturation range.

From equation (3) it can be seen that the displacement of an individual saturation value is proportional to F'_w, where F'_w is the derivative of the fractional flow function with respect to the saturation. Typical curves of the fractional flow function F_w and its derivative F'_w are shown in Fig. 4. These curves are characteristic of the early stages of infiltration when V is large and counterflow is not yet occuring. Now if all saturations are initially available at the surface, the saturation profile will assume a shape similar to that shown in Fig. 5. Because of the proportionality between z_{S_w} and F'_w in equation (3) the shape of the saturation profile is essentially the same as that of F'_w vs S_w.

It is apparent from Fig. 5 that the saturation is not single valued for all values of z. Since this is not physically reasonable, the application of equation (3) will need to be modified to some degree. Buckley and Leverett (1), who originally developed equation (3), suggested the construction of a front whose position was determined by means of a material balance. A construction of this type is shown in Fig. 6. The material balance is attained when the two cross-hatched areas in the figure are equal. The material balance is important in that it provides a means

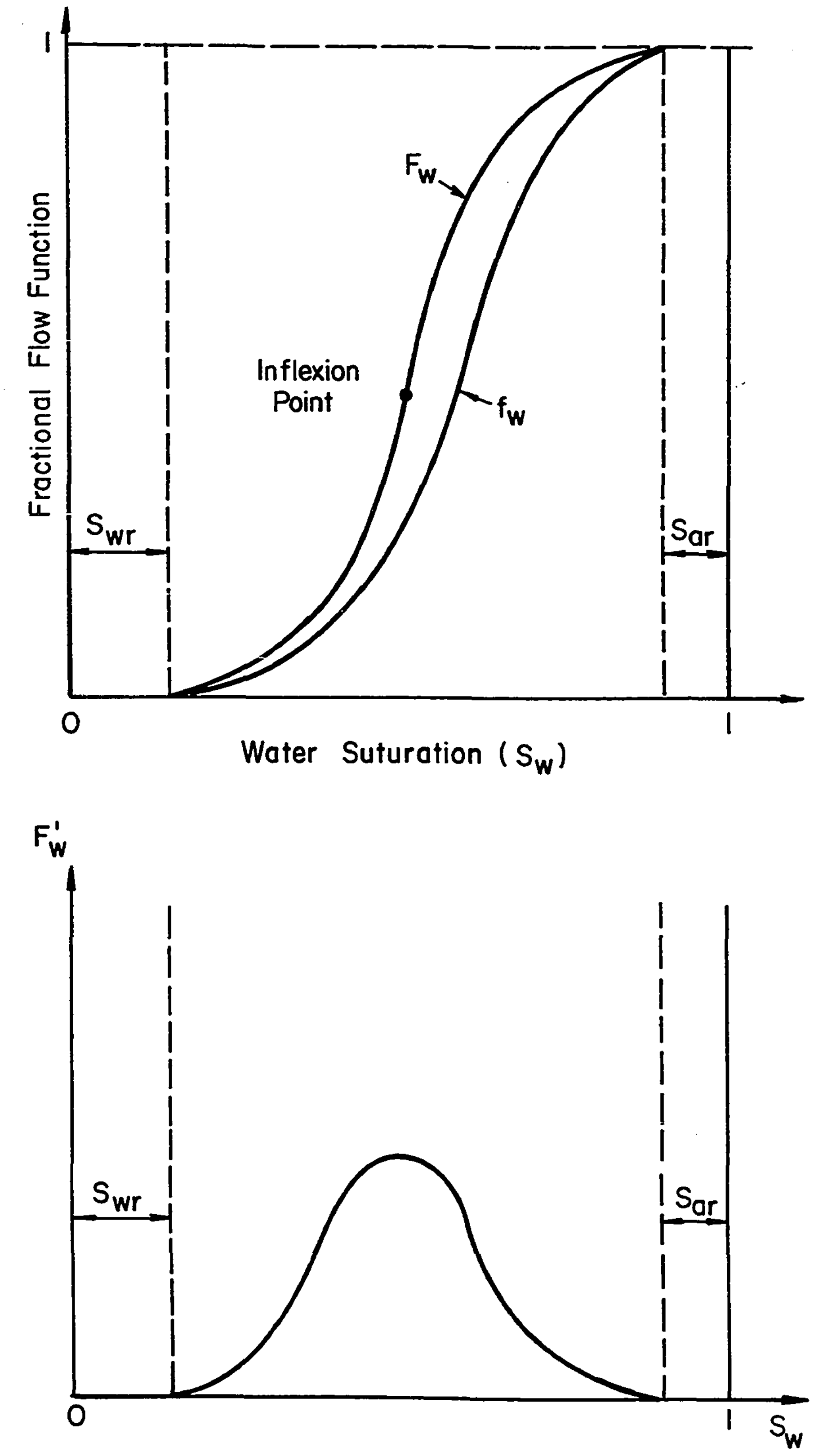

Figure 4 Fractional Flow Function and Derivative

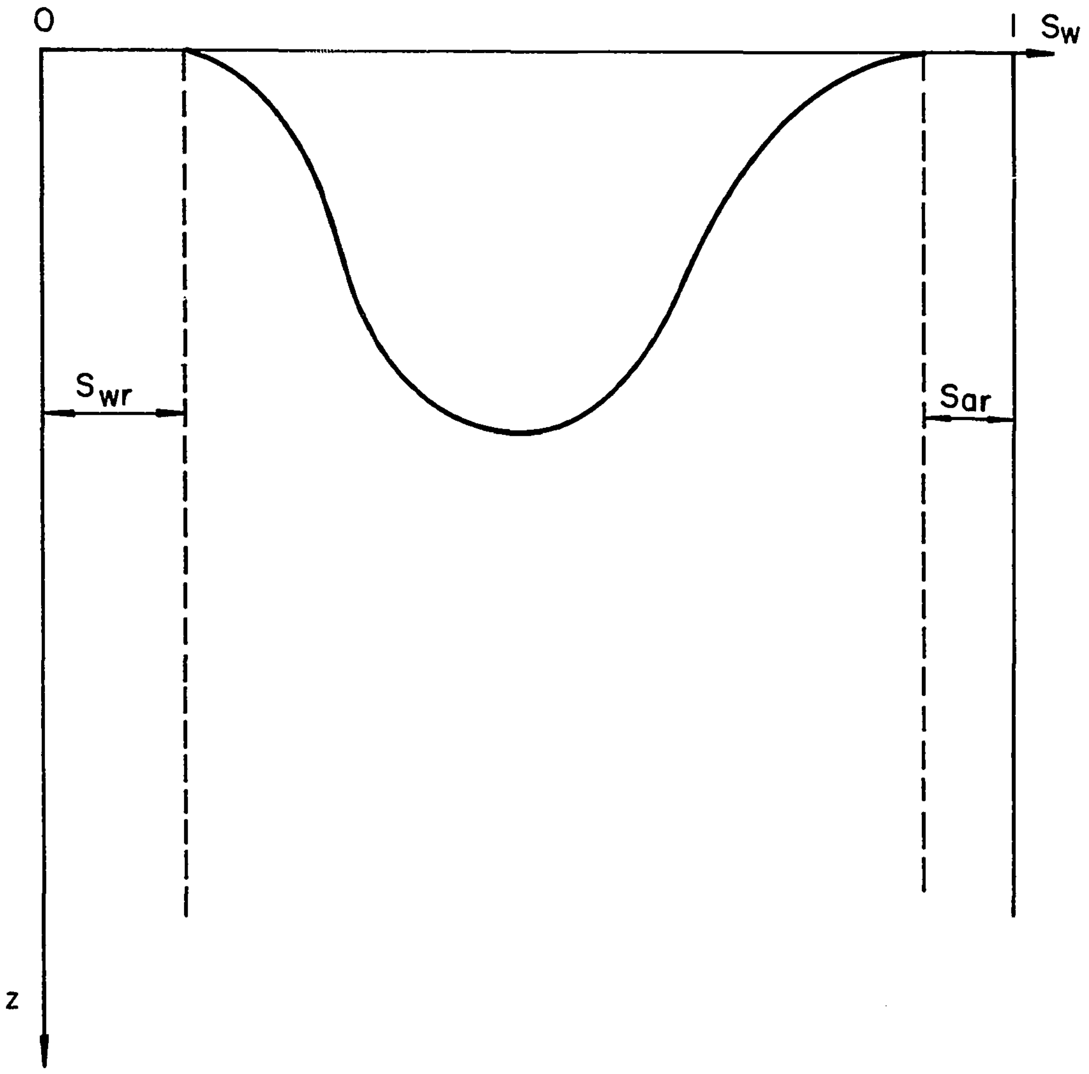

Figure 5 Saturation Profile as Predicted by Equation (3)

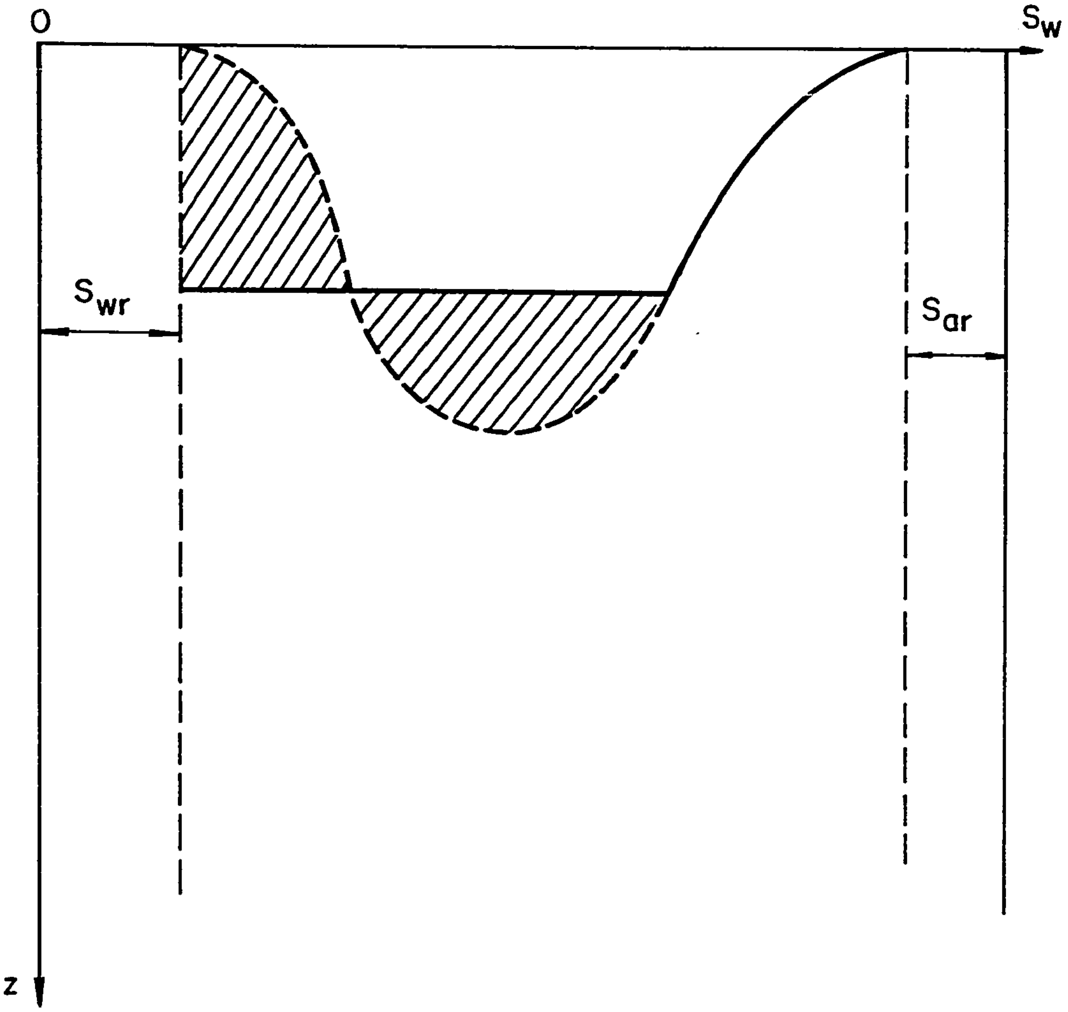

Figure 6 Saturation Profile Based on Buckley-Leverett Construction

whereby the area under the saturation profile will remain unchanged by the construction of a front.

A later development by Welge (23) offers a graphical technique for determining the position of the front when the initial saturation is uniform. If a front is to be maintained, all of the saturations along the front must necessarily move with the same velocity. This would be the case if the F_w curve were replaced by a straight line over the saturation range covered by the front, that is, F'_w and consequently the velocity of each saturation would then be the same. Conversely, a straight line approximation between any two points on the F_w curve (a secant) will result in the formation of a front between the same two saturation points on the saturation profile. It can also be shown (Appendix 1) that any straight line approximation on the F_w curve will yield a material balance on the saturation profile. The actual position of the secant construction will be based on two criteria: the saturation must be a single valued function of z, and the solution given by equation (3) is to be preferred over the approximate solution wherever the result is still physically meaningful. Fig. 7 illustrates the required construction and the corresponding saturation profile. Note that the construction extends from the initial saturation to a point that is tangent to the F_w curve. A construction in any other position would violate one of the two previously mentioned criteria.

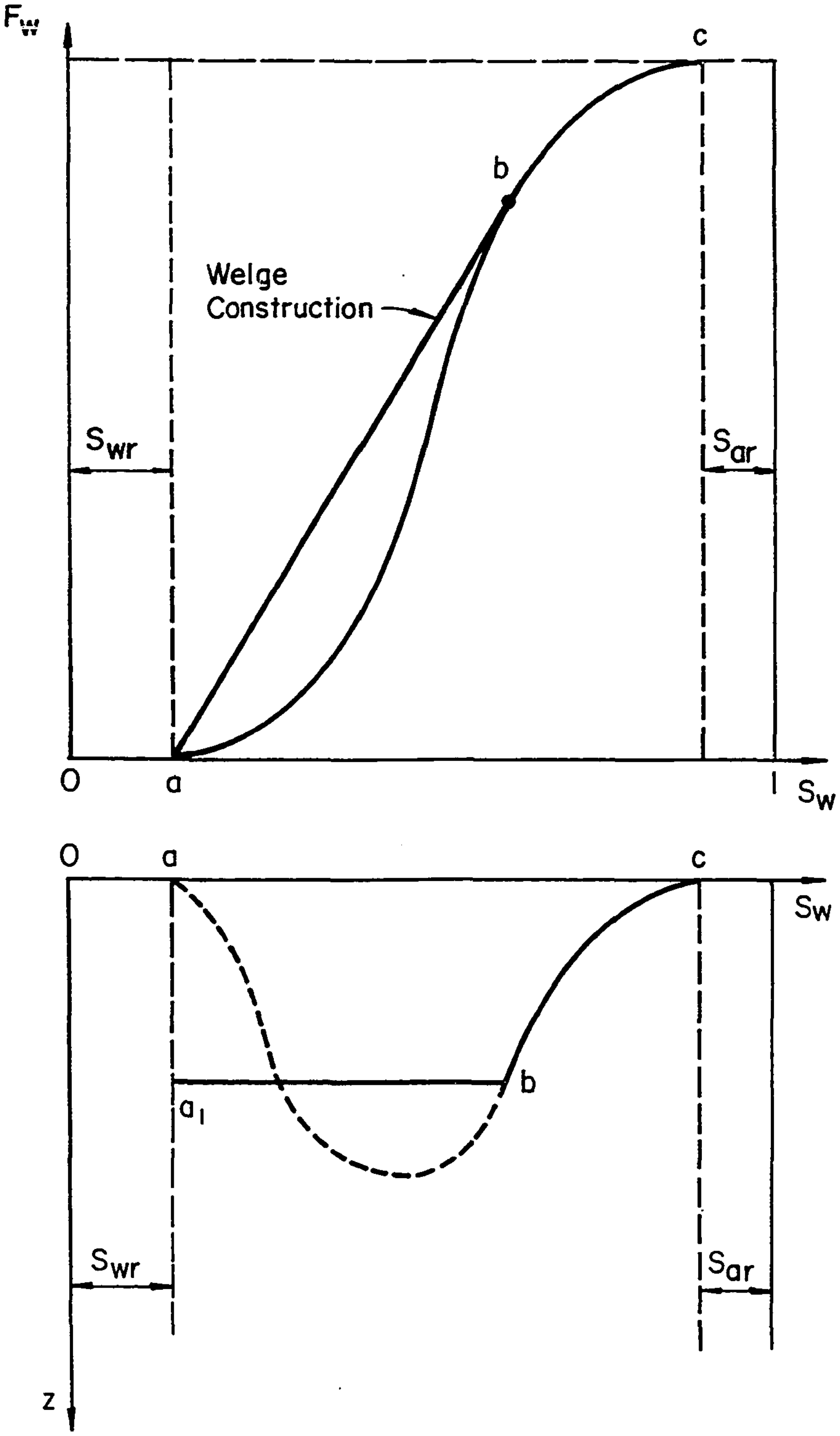

Figure 7 Welge Front Construction

With the secant approximation to the F_w curve, all of the saturations in the front will be displaced an equal amount. The displacement will be proportional to the slope of the secant. Saturations beyond the point of tangency of the secant will be displaced a distance proportional to the slope of the F_w curve at that particular saturation value. A consideration of equation (8) indicates that the shape of the F_w curve, and hence the position of the secant, will change as V changes. However the previously described technique provides a means of determining the secant position and the corresponding saturation profile for each new value of V.

As the infiltration progresses the total velocity may decrease to a value that permits counterflow. If this occurs, the fractional flow function and the saturation profile will take forms similar to those in Fig. 8. The solid lines in Fig. 8 represent the conditions before counterflow, and the dashed lines represent conditions after counterflow. Recalling that the displacement of a saturation value is proportional to the slope of the F_w curve, an examination of the dashed F_w curve reveals that for one saturation value, S_{w_o} , the slope is zero. All saturation values lower than S_{w_o} have a positive slope and will continue to move downward. However at saturations greater than S_{w_o} , the slope is negative and consequently these saturations move up.

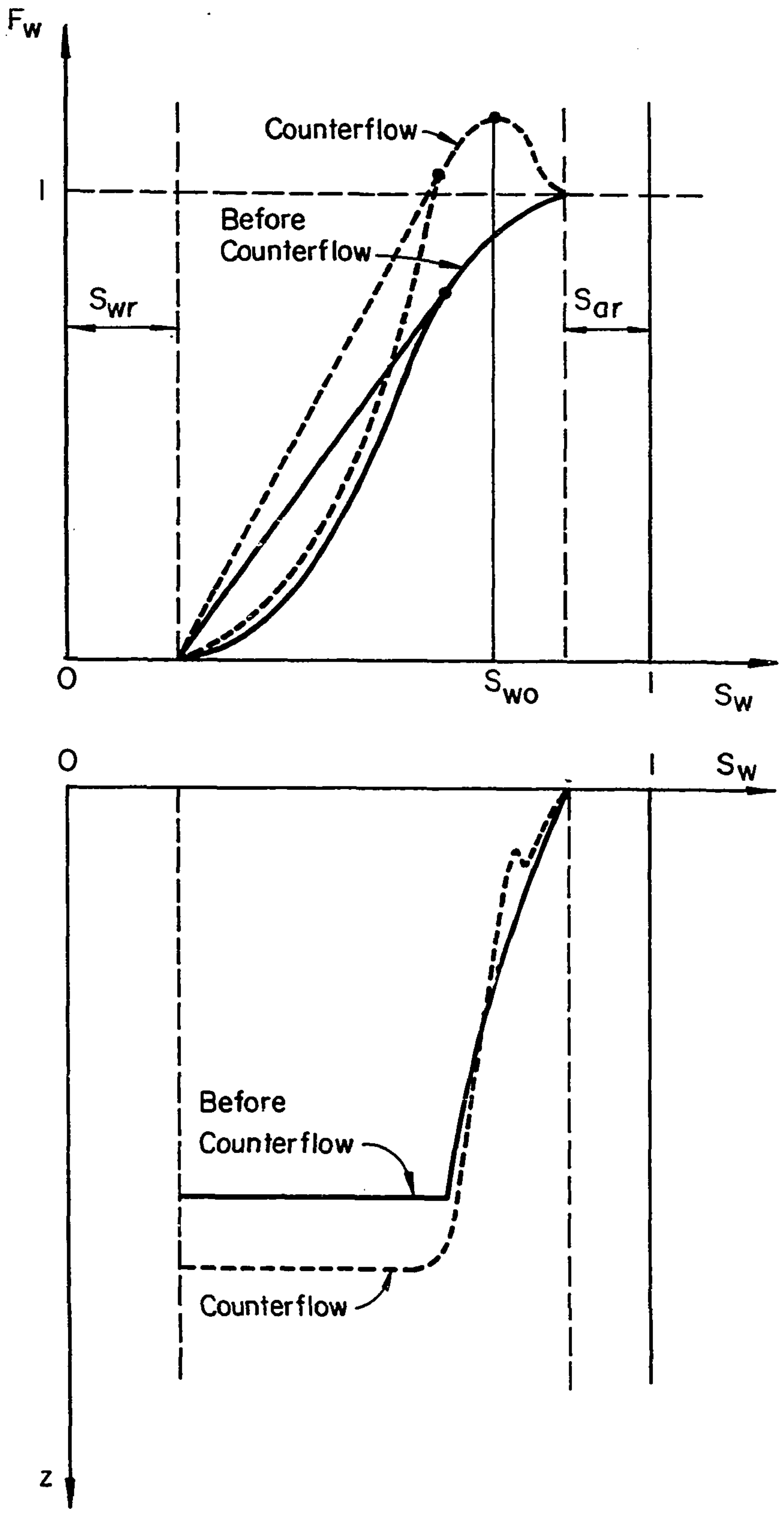

Figure 8 Fractional Flow Function and Saturation Profile as Counterflow Commences

It is evident in Fig. 8 that the saturation becomes a multiple valued function of z in the upper saturation range. Since this is not physically acceptable, a secant construction is again employed to eliminate the multiple values. Unlike the previous situation requiring a secant approximation, this multiple-valued portion of the saturation profile did not develop from an initially uniform saturation. As a result there is a transition stage during which a Buckley-Leverett type front develops. Morel-Seytoux (25) describes a means whereby a material balance is used to establish the position of the front as it grows. After the front becomes fully developed, a construction like that due to Welge can be used again. In this study it is assumed that the Welge approximation is valid from the beginning of counterflow. A rigorous treatment of the short-lived transition stage is not thought to be warranted in view of the other approximations already made. It should also be noted that only a limited part of the profile would be changed by the more rigorous approach. The material balance condition will still be maintained by the simpler Welge approximation. Fig. 9 shows conditions before and after counterflow when the Welge construction is employed.

The fractional flow function concepts which have been discussed up to this point are those that are likely to be encountered in a majority of problems. Some additional concepts will be discussed in connection with the

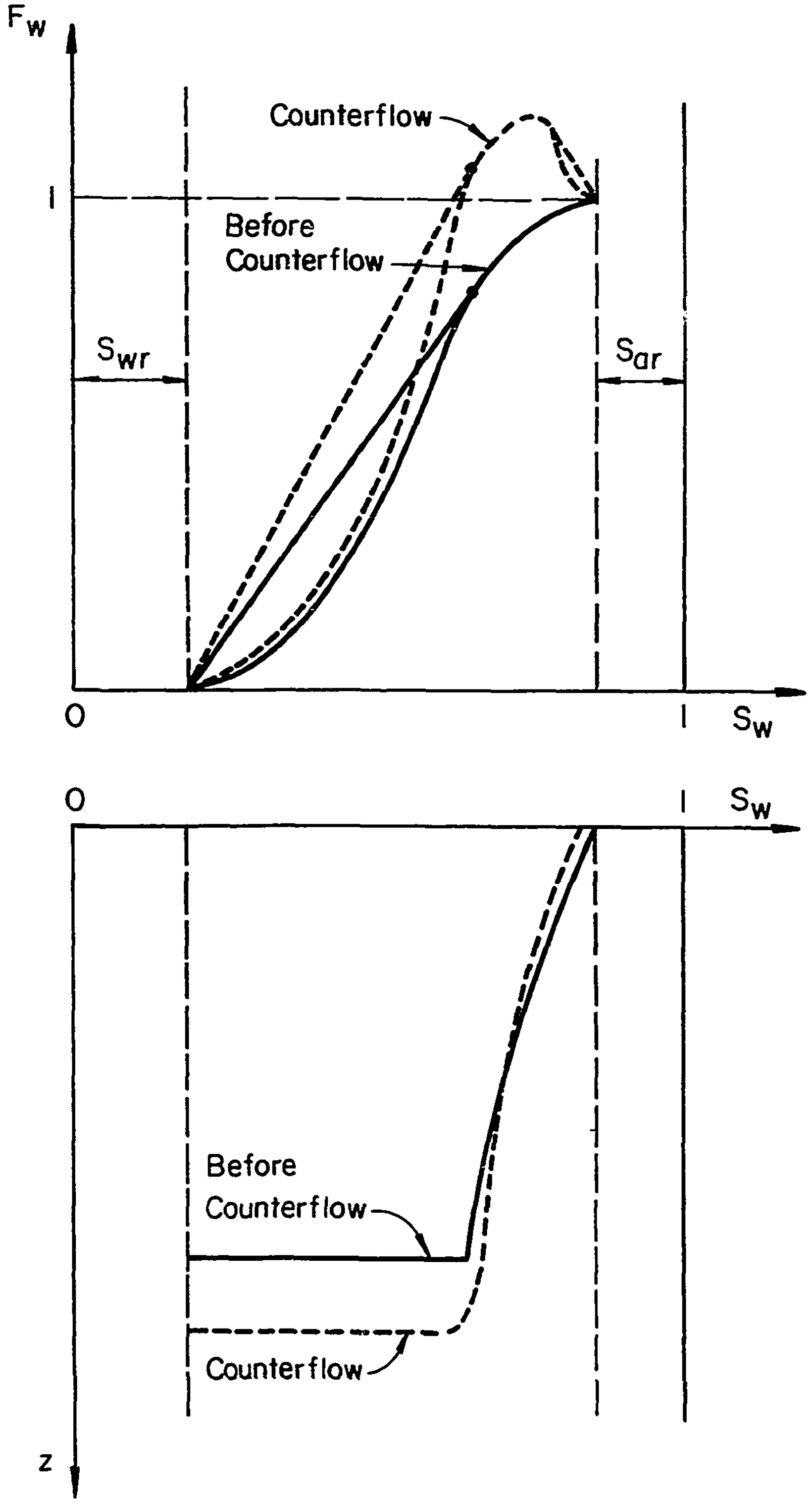

Figure 9 Counterflow of Air with Welge Approximation

special problems to which they are peculiar.

At any time t the determination of the fractional flow function depends upon a knowledge of the total velocity V. This can be seen from equation (8). As previously mentioned, the integral equation (4) provides the necessary relationship for the computation of V.

3.2 The Integral Equation

The development of equation (4) from Darcy's law and the capillary pressure relationship is detailed in Appendix 1. Equation (4) is

$$-\int_1^2 dp_w + \int_1^2 \rho_w g dz = V\int_1^2 \frac{dz}{k\left(\frac{k_{ra}}{\mu_a} + \frac{k_{rw}}{\mu_w}\right)}$$

$$+ g(\rho_w - \rho_a)\int_1^2 (1-f_w)dz + \int_1^2 (1-f_w)dp_c \qquad (4)$$

This equation can be modified somewhat to a form which better lends itself to numerical computations. The modified form also provides a clearer understanding of the important factors which influence the total velocity.

At atmospheric conditions the density of water is approximately 1,000 times that of air. However, in a porous medium air may become entrapped and compressed by infiltrating water. If this were to occur, and if the pressure in the air were to be increased to twice atmospheric pressure (an unlikely event since buoyant forces tend to move the air up through the water), the density of water would still be 500 times that of air. Following this reasoning, the neglect of ρ_a in the term $(\rho_w - \rho_a)$ should have a minimal effect on the computation of V. The density of air will therefore be neglected in equation (4).

For immiscible fluids the relationship between the pressure in the water and the pressure in the air is

$$p_c = p_a - p_w$$

or in a differential form and rearranged:

$$dp_w = dp_a - dp_c$$

Incorporating these changes, expanding and rewriting equation (4) yields

$$-\int_1^2 dp_a + \int_1^2 dp_c + \int_1^2 \rho_w g dz = V\int_1^2 \frac{dz}{k\left(\frac{k_{ra}}{\mu_a} + \frac{k_{rw}}{\mu_w}\right)}$$

$$+ \int_1^2 g\rho_w dz - g\rho_w \int_1^2 f_w dz + \int_1^2 dp_c - \int_1^2 f_w dp_c$$

A combination and further rearrangement of terms gives

$$V = \frac{-\int_1^2 dp_a + g\rho_w \int_1^2 f_w dz + \int_1^2 f_w dp_c}{\int_1^2 \frac{dz}{k\left(\frac{k_{ra}}{\mu_a} + \frac{k_{rw}}{\mu_w}\right)}} \qquad (9)$$

It is evident from equation (9) that the value of V at any time will depend upon the saturation profile at that time. As previously explained, the profile to be used in the computation of V for a given time interval will be that profile which existed at the end of the previous time interval.

Each of the integrals on the right side of equation (9) must be evaluated in order to determine V. The means by which the integrals are to be evaluated is discussed in the following paragraphs. The limits of integration will be from a point immediately below the ground surface to a point immediately ahead of the advancing front.

The effect of increased pressure in the air entrapped by the incoming water is felt through the integral $-\int_1^2 dp_a$, which may be integrated to give

$$-\int_1^2 dp_a = p_{a_1} - p_{a_2}$$

The pressure immediately below the surface p_{a_1}, can be obtained from the capillary pressure relationship:

$$p_a = p_c + p_w$$

The term p_w represents the pressure in the water at the ground surface and will depend upon the depth of water ponding H, and the atmospheric pressure p_A. The magnitude of p_c will depend upon the saturation at the surface, a quantity which will be known from the saturation profile, and the experimentally obtained relationship between capillary pressure and water saturation. A typical capillary pressure curve is shown in Fig. 10. Finally, the pressure in the air at the ground surface is given by

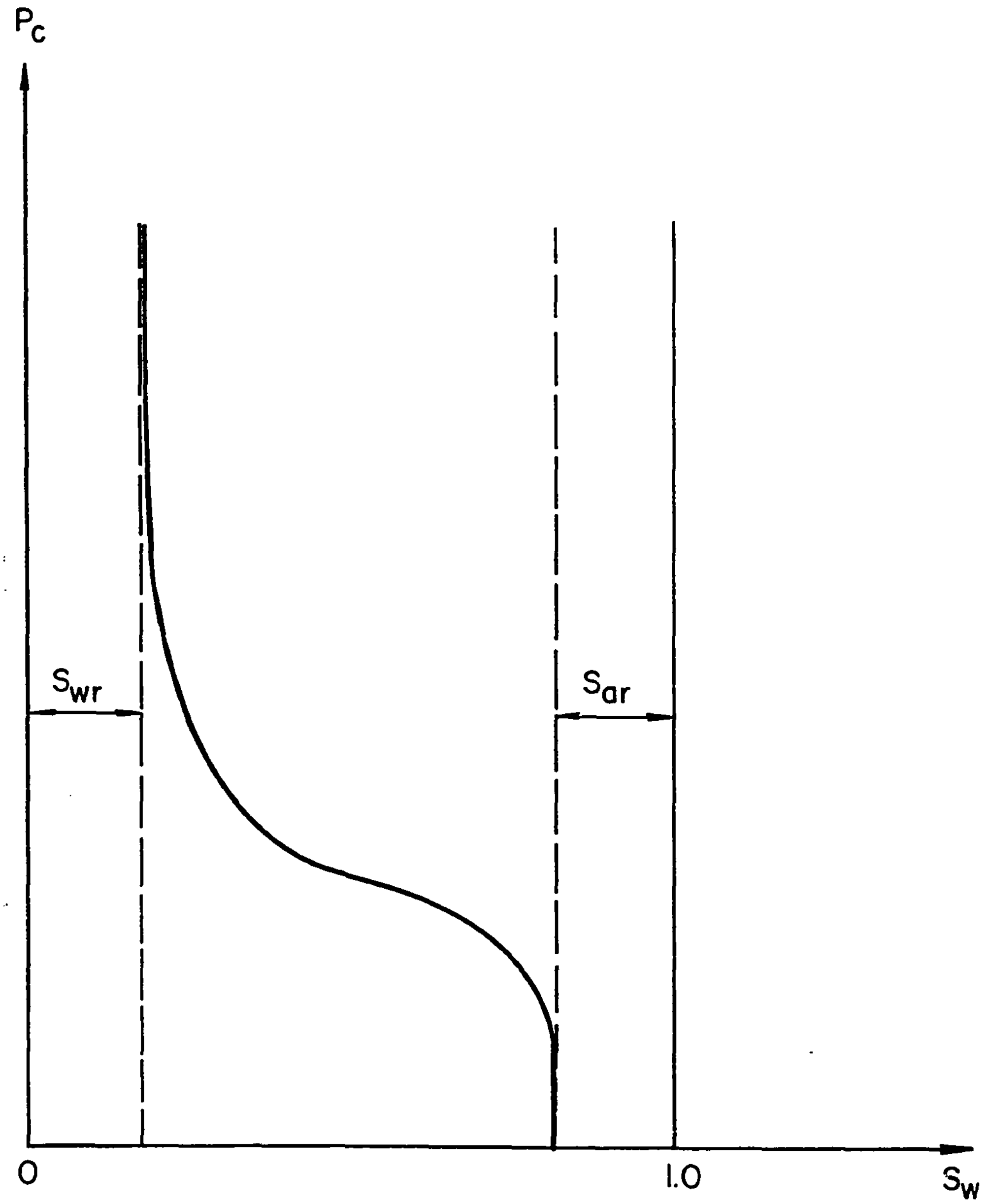

Figure 10 Typical Curve of Saturation Versus Capillary Pressure

$$p_{a_1} = p_c + \rho_w gH + p_A$$

If the air is assumed to behave like a perfect gas, the air pressure ahead of the front, p_{a_2}, can be determined by the perfect gas law:

$$p_{a_2} = p_2 = \frac{p_1 v_1}{v_2}$$

where the subscript 1 denotes conditions before infiltration begins and 2 denotes conditions at some later time. The quantity p_1 will be atmospheric pressure, while the volumes v_1 and v_2 will depend on the initial and current saturation profiles and the water table depth. This relationship will satisfactorily determine p_{a_2} until such time as counterflow occurs. Then it will be necessary to account for that portion of the entrapped air which escapes at the surface. The rate at which air escapes during a given time interval can be obtained from the definition of the total velocity,

$$V = V_a + V_w$$

where V and V_w have been previously determined.

The integral expression $g\rho_w \int_1^2 f_w dz$ in equation (9) reflects the effects of gravity as a driving force for infiltration. The evaluation of this integral requires a numerical integration. With this integral expression, as with those remaining in equation (9), a graphical representation provides an aid in visualizing the numerical integration which is to be performed. From a consideration of the fractional flow function curve (f_w vs S_w) and the saturation profile (z vs S_w), the appearance of the f_w vs z curve can be deduced. Fig. 11 illustrates the general shape of this curve.

The influence of capillarity on the total velocity V is felt through the integral $\int_1^2 f_w dp_c$. Here again, evaluation of the integral requires a numerical integration. The graphical representation of this integral can be obtained from a consideration of the fractional flow function curve (f_w vs S_w) and the capillary pressure curve (p_c vs S_w). A typical curve is shown in Fig. 12. Note that as f_w approaches zero, p_c approaches infinity. Fig. 10 shows that this is a result of p_c approaching infinity as the saturation approaches its residual value - i.e. - that saturation value at which the mobility of water becomes zero. However, laboratory techniques are incapable of detecting exactly when residual saturation is reached. As a result, experimental data can only provide some high finite value of capillary pressure as that corresponding to residual saturation. In view of the dependence upon experimental capillary data in this study, the value of f_w , in Fig. 12, will be considered to go to zero at some finite value of capillary pressure.

The remaining integral in equation (9) reflects the resistance to flow. This integral, which is

$$\int_1^2 \frac{dz}{k\left(\frac{k_{ra}}{\mu_a} + \frac{k_{rw}}{\mu_w}\right)}$$

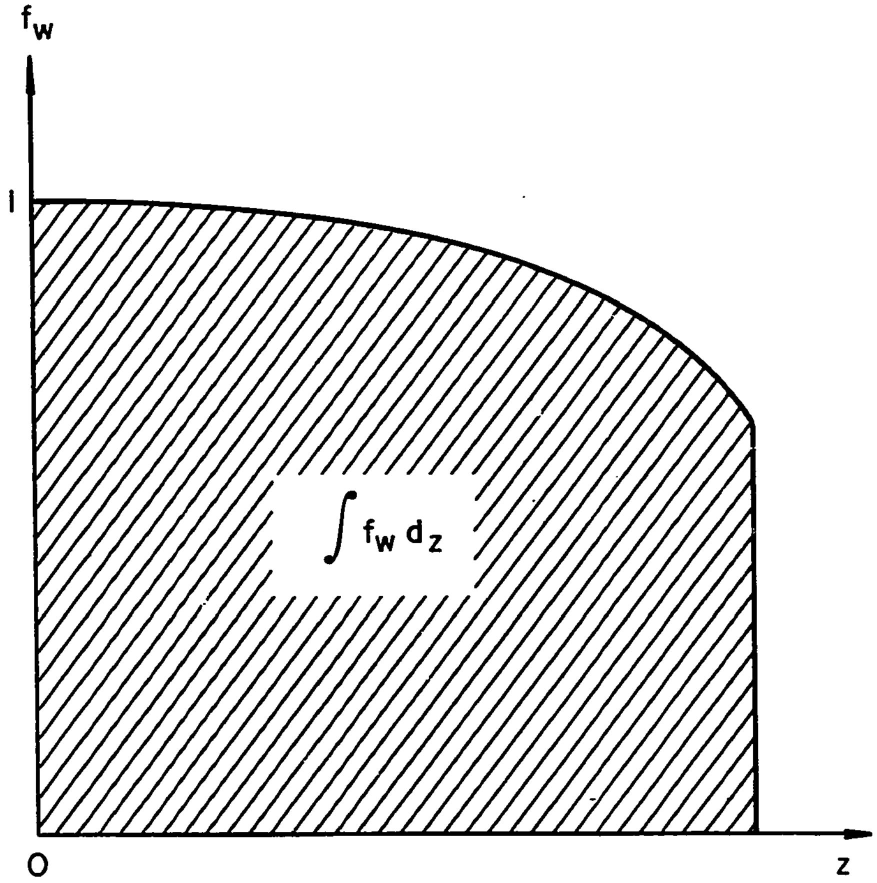

Figure 11 Graphical Representation of the Integral $\int f_w dz$

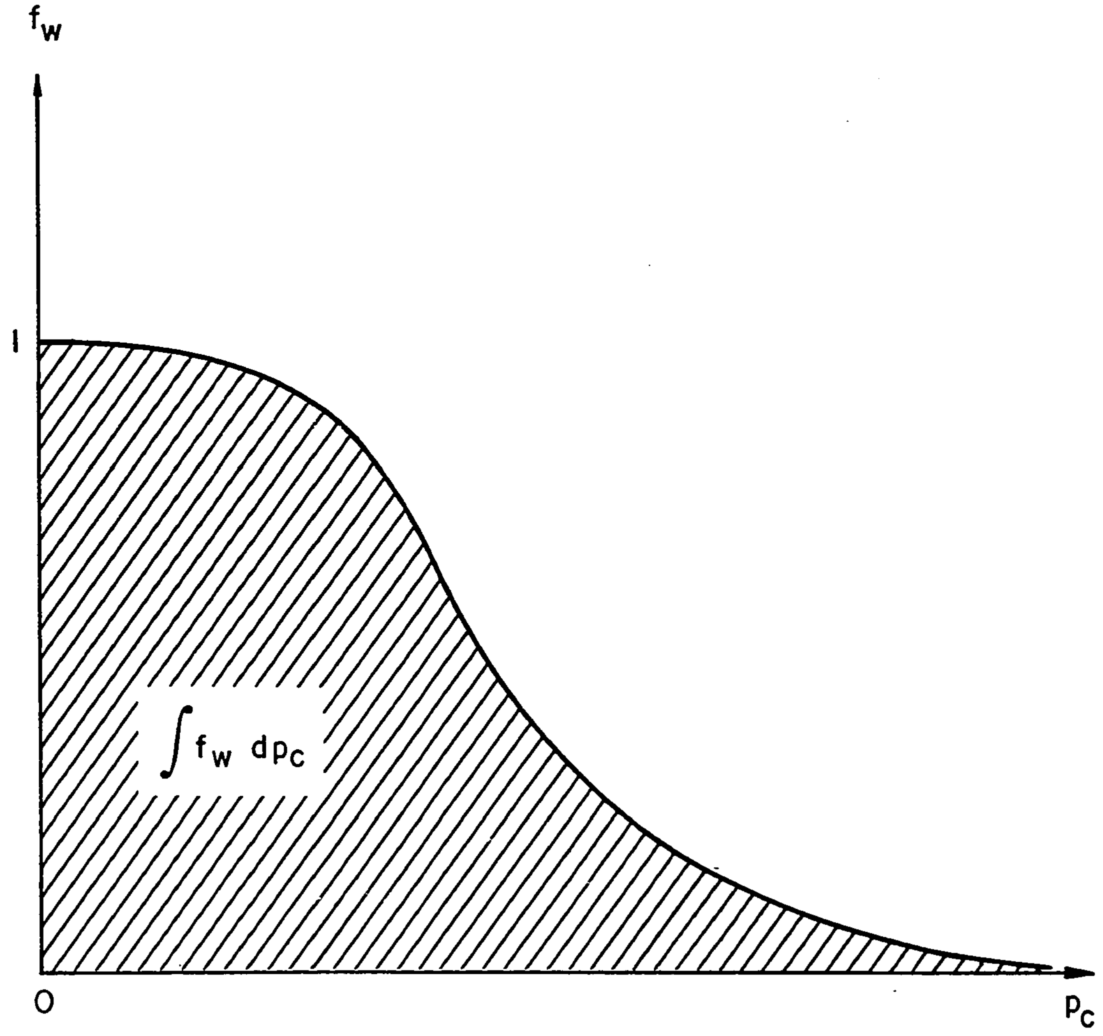

Figure 12 Graphical Representation of the Integral $\int f_w dp_c$

must also be evaluated by numerical procedures. The graphical form of this integral can be deduced from an examination of the two relative permeability curves (k_{ra} vs S_w and k_{rw} vs S_w) and the saturation profile (z vs S_w). The general shape of the curve is shown in Fig. 13.

The solution and subsequent substitution into equation (9) of each of the above mentioned integrals provides a means of determining the total velocity V based on the previously computed saturation profile. This V will then be used in conjunction with equation (3) and the Welge approximation to determine the new saturation profile at the end of the next time increment and so on. As previously stated, these two general operations provide the basis for the computational scheme to be followed in the determination of infiltration quantities.

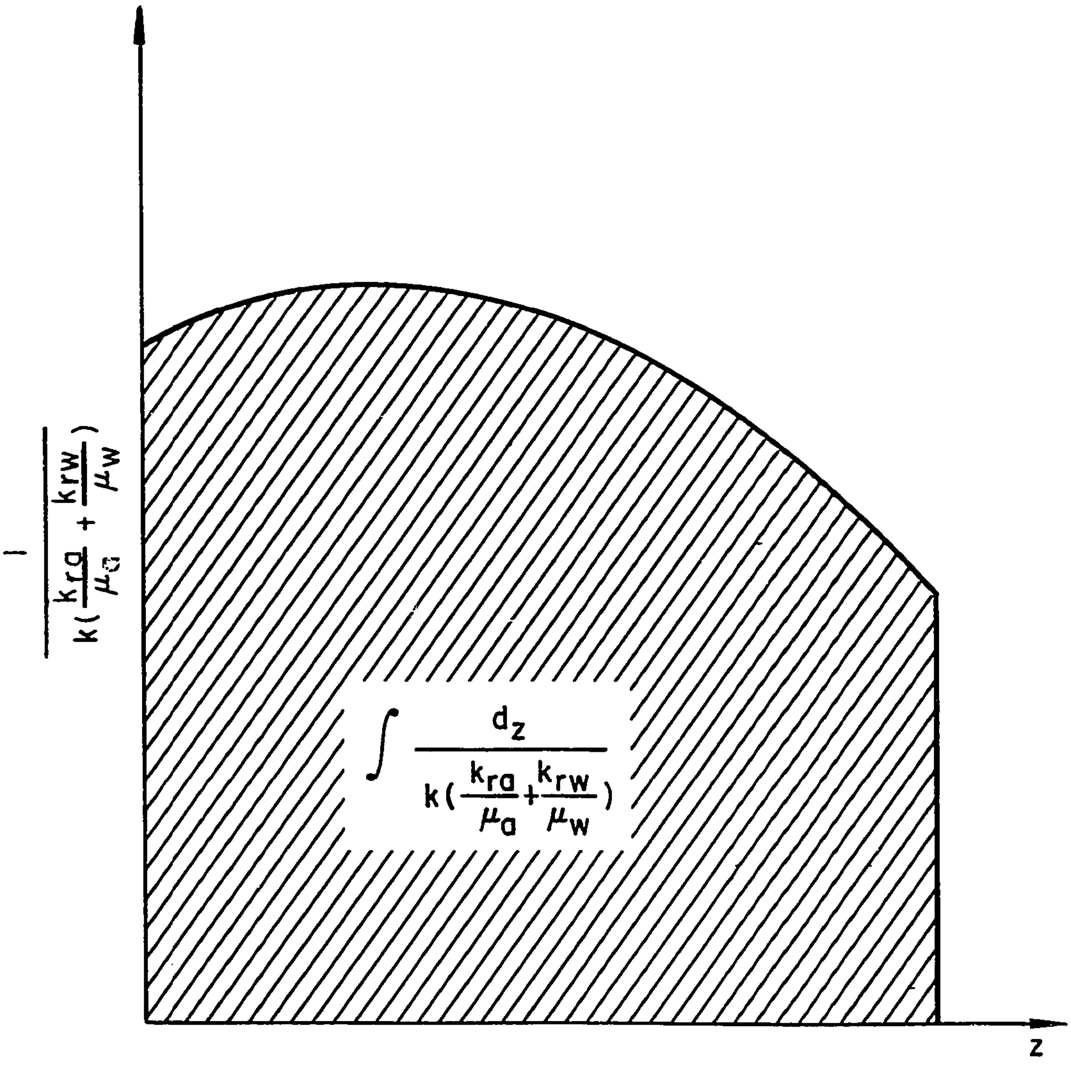

$\frac{1}{k(\frac{k_{ra}}{\mu_a}+\frac{k_{rw}}{\mu_w})}$
$\int \frac{d_z}{k(\frac{k_{ra}}{\mu_a}+\frac{k_{rw}}{\mu_w})}$
z

Figure 13 Graphical Representation of the Integral $\int \frac{d_z}{k(\frac{k_{ra}}{\mu_a}+\frac{k_{rw}}{\mu_w})}$

Chapter 4

DATA USED FOR STUDY

A number of the equations employed in this study are dependent for their application upon a knowledge of various soil properties. The relationships between capillary pressure and saturation, between relative permeability of air and saturation, and between relative permeability of water and saturation must be known. In addition, the porosity and the intrinsic permeability of the soil must be known. This type of soil information is usually obtained experimentally. However, since this is not an experimental study, it was necessary to acquire the needed soil data by other means.

The literature, which is the most obvious source of soil data, failed to provide the desired information completely. It was found that although there is ample soil data from a variety of experimental studies published, there is a definite lack of comprehensive data about any single soil. This is because, for the most part, the experimental studies were unrelated in the sense that each study was primarily concerned with a particular aspect of porous media flow in a particular soil.

Since the required soil information could not be obtained from the literature, hypothetical soils with appropriate soil parameters and relationships were utilized. Actually, the soil data that was used most extensively as the basis for analysis, was not assumed in its entirety, but only in part. Experimental results from a Ph.D thesis by Brooks (26) were used and modified only to the extent necessary to make them suitable to the needs of this study. This was done in an effort to insure that the soil information would be as realistic as possible. This modified soil data is illustrated graphically in Figures 32 and 33 of Appendix 2. Additional hypothetical soil data, from a thesis by Le Van Phuc (27), was used less extensively. This data is shown in Figures 34 and 35 of Appendix 2.

Chapter 5

ANALYSIS AND RESULTS

In this chapter the previously described hypothetical soils are subjected to several different sets of boundary and/or initial conditions and then analyzed. Computer programs were written to perform the analysis for each situation. The programs are designed to investigate the evolution of the saturation profile and the variation of the infiltration rate with time. The various boundary value problems are treated separately in the following sections.

5.1 Case (1)

In this first situation the initial water saturation is assumed to be uniform and equal to the residual water saturation. At the upper surface it is assumed that water is ponded to a constant depth of 5 cm throughout the duration of the infiltration process. The medium is considered to be semi-infinite in extent, so that there are no conditions imposed at the lower boundary. The conditions just described might be approached in the field when a soil with a very deep water table was irrigated by flooding, or subjected to intense rainfall, after an extended period without irrigation or precipitation.

The treatment of this particular problem varies only slightly from the general treatment detailed in Chapter 3. As before, the Buckley-Leverett equation and the integral equation provide the means for determining the saturation profile at any time t. However, under these boundary conditions, not all of the terms in the integral equation vary with each time step. The term p_{a_2}, which represents the pressure ahead of the advancing front, remains constant throughout the infiltration process. It is initially atmospheric and remains atmospheric because of the semi-infinite extent of the medium.

The results of a computer analysis of this problem are illustrated in Figures 14 through 16. Figure 14 shows how the saturation profile advances into the soil with time. The movement of the water into the soil is almost piston-like, in that almost all of the mobile air behind the advancing front has been displaced by water. That portion of Figure 14 in the saturation range between 0.880 and 0.940 has been enlarged and reproduced in Figure 15. This was done to better illustrate the way in which the saturation profile near the surface shifts as a result of the counterflow of air. It can be seen in Figure 15 that the saturation at the surface remains equal to the residual saturation of air, S_{ar}, at 5.86 hours after infiltration has commenced. This indicates that no air has escaped at the surface up to this time. However, after 139.20 hours, the saturation at the surface has decreased to a value less than S_{ar}. This implies that between 5.86 hours and 139.20 hours counterflow of air has begun to occur. Consideration of the remaining profiles demonstrates the way in which the saturation profile continues to change as the counterflow of air increases.

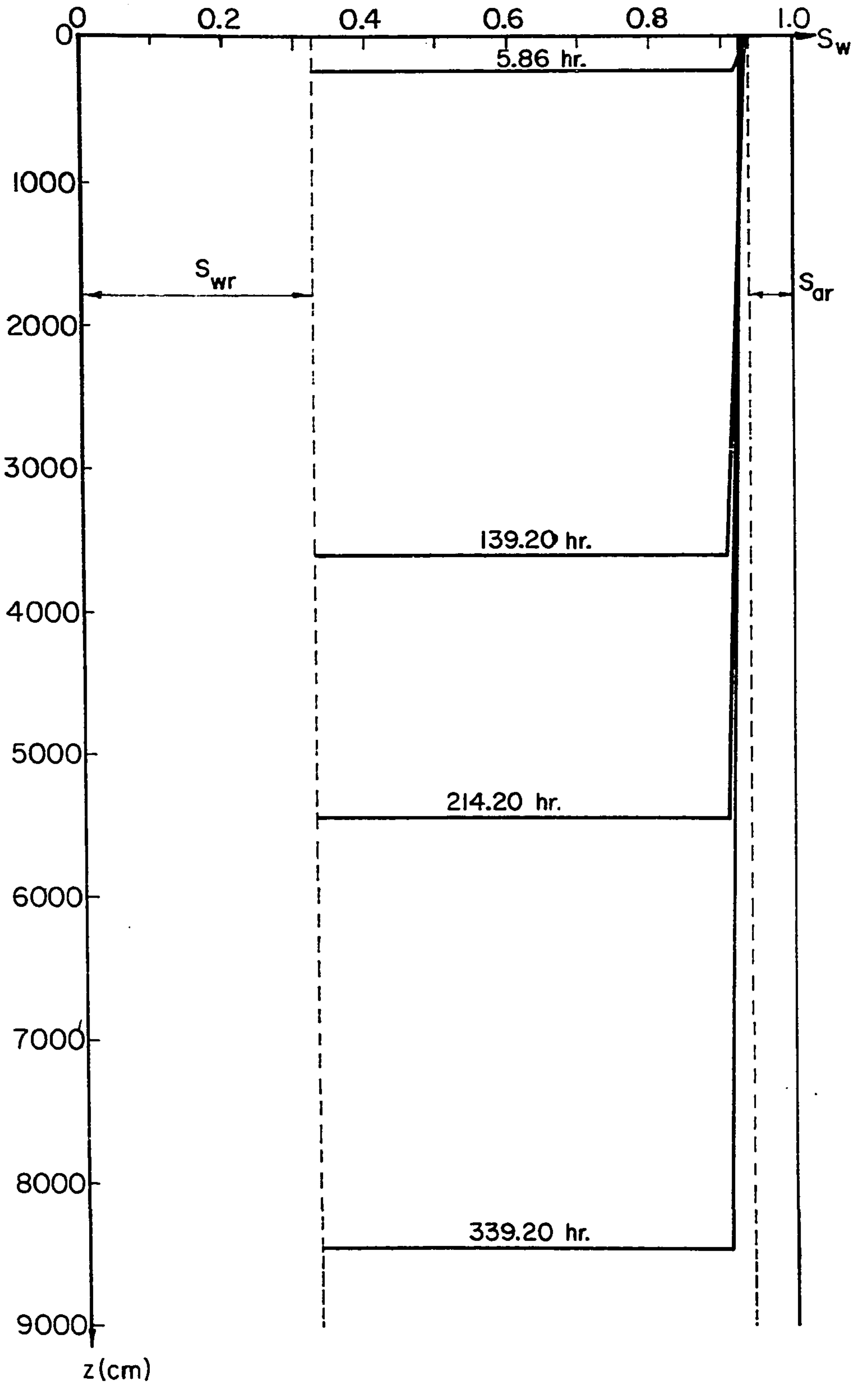

Figure 14 Advance of the Saturation Profile in a Semi-infinite Medium (Medium Characteristics are Shown in Figure 32 and 33 of Appendix 2)

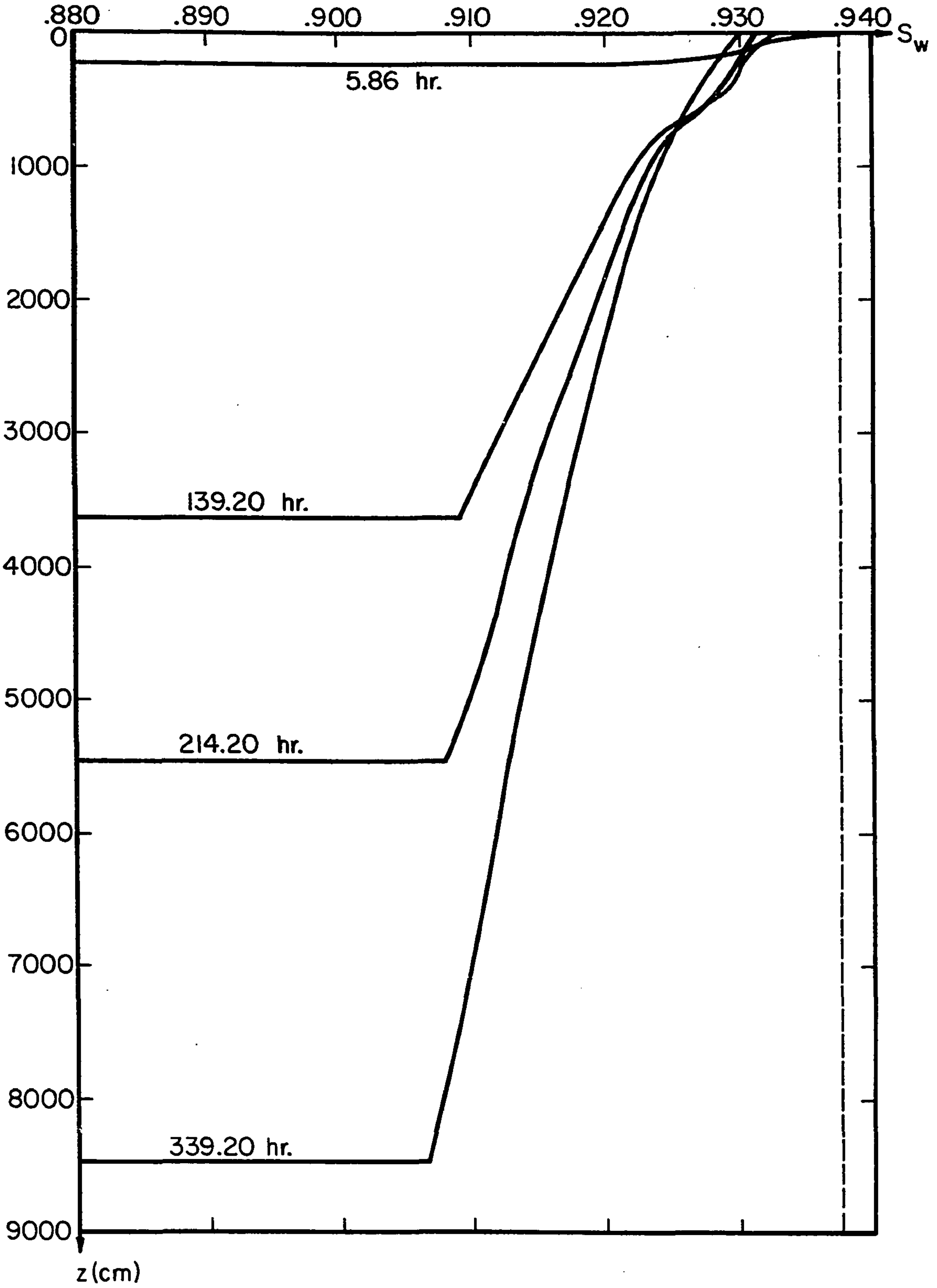

Figure 15 Advance of the Saturation Profile in a Semi-infinite Medium (Enlargement of a Section of Figure 14)

In the semi-infinite medium the air counterflow occurs as a result of a back pressure in the two-phase flow region. Figure 13 illustrates that at some depth within this region a maximum resistance to the total velocity exists. As the resistance to the total velocity increases toward the maximum, the pressure gradient must increase in order to maintain a constant velocity. Thus, the back pressure, which is necessary for the occurrence of counterflow, develops. Although the existence of a back pressure does not, in itself, guarantee a counterflow, it is evident from Equation A2 of Appendix 1 that the back pressure in the air phase, $\frac{\partial p_a}{\partial z}$, need not be too large to overcome $\rho_a g$, and cause V_a to be negative.

Figure 16 shows how the infiltration rate and the cumulative infiltration vary with time. It can be seen that the infiltration rate is initially very high. This is to be expected, since an initial water saturation, which is residual, and a saturation profile, which has just begun to enter the soil, combine to produce an extremely large capillary pressure gradient $\frac{\partial p_c}{\partial z}$. However, as the profile advances farther into the soil, the magnitude of this gradient decreases rapidly causing the infiltration rate to also decrease rapidly. As more water enters the soil, the effect of gravity as a driving force for infiltration increases. The resistance to flow also increases as additional water enters the soil. As the relative importance of these factors continue to change, the infiltration rate levels

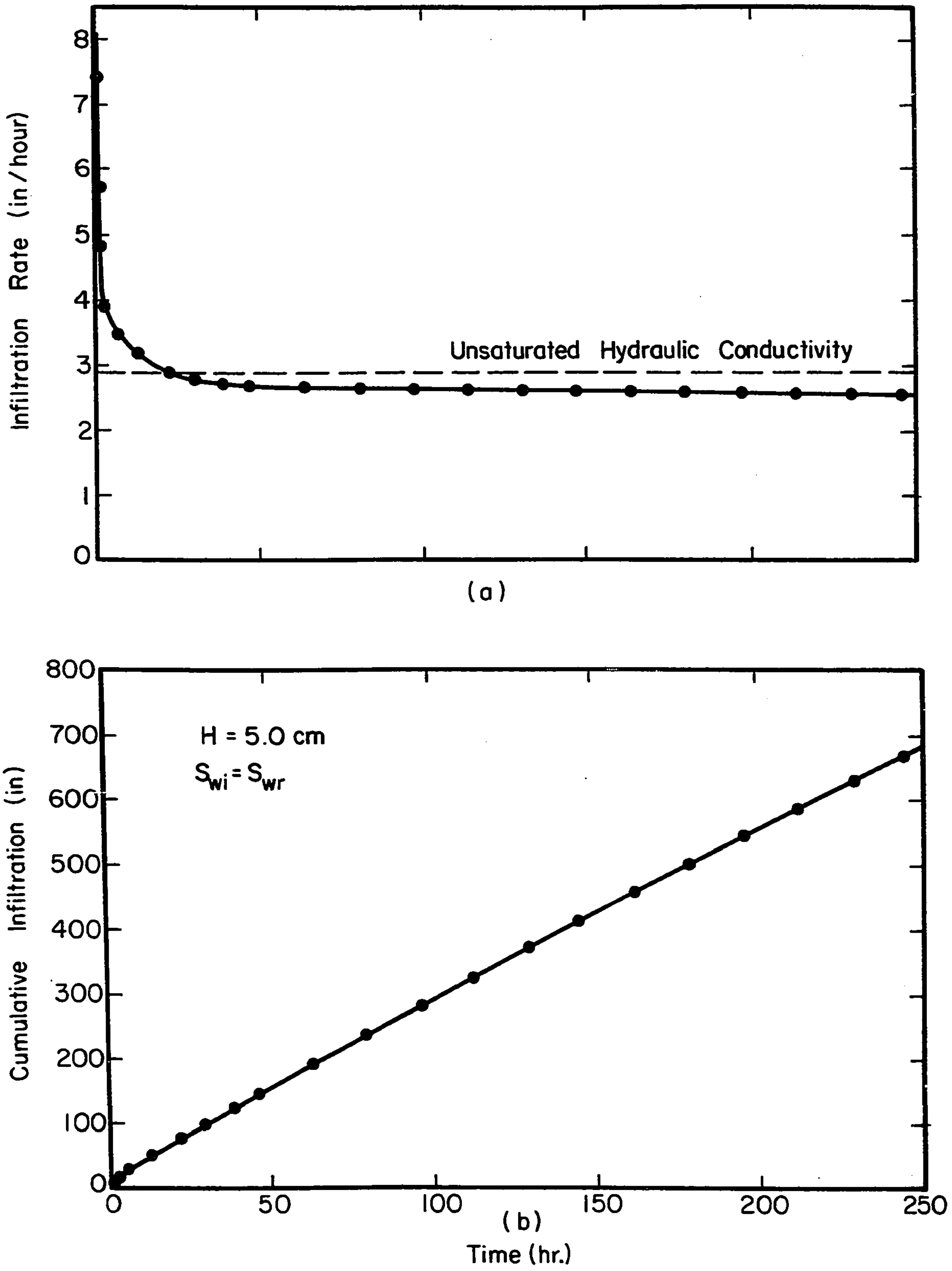

Figure 16 Infiltration Rate versus Time and Cumulative Infiltration versus Time for a Semi-infinite Medium (Medium Characteristics are Shown in Figures 32 and 33)

off and approaches a constant value asymtotically. The value approached is something less than the unsaturated hydraulic conductivity of the soil. This is reasonable because air is flowing through the soil in a direction opposite to the flow of water. Thus, the flow of water must be expected to occur at a lower rate than it would if no air were present in the flow region.

The cumulative infiltration is illustrated in (b) of Figure 16. In both (a) and (b) of Figure 16, it can be seen that the calculated points fall on smooth curves. Although individual data points have not been represented on all of the figures in the remainder of this paper, this same smoothness of results was observed in all cases.

5.2 Case (2)

The boundary condition at the upper soil surface, and the initial moisture condition are the same as in the first case. However, it is not now supposed that the medium is of a semi-infinite extent. Instead, a water table is assumed to exist at a depth of 150 cm. Although the presence of a water table and the condition of a uniform initial saturation are not entirely consistent, the situation might be approached with a soil in which the capillary fringe was of a limited extent.

The presence of a water table at a reasonable depth makes it necessary to consider the pressure build up in the air trapped between the advancing front and the water table. The computational procedure for evaluating the pressure increase in the entrapped air is outlined in Chapter 3.

What is the effect of the pressure build up on the infiltration process? Equation (9) reveals that it tends to reduce the total velocity, and in so doing, retards the downward moving saturation profile. The increased pressure also causes counterflow of air to begin much more quickly and to progress much more rapidly than in the case of the semi-infinite medium. This increasing counterflow means that V_a is becoming larger in a negative sense. As a result, V is further decreased. After a certain period of time, which varies with the water table depth, the total velocity V reaches zero. At this time air is escaping from the medium at the same rate at which water is entering. Consequently, no further compression of the entrapped air will occur.

Actually, although the total velocity approaches zero, it is not allowed to take on a zero value in the computational procedure. The reason for this can be seen by considering the definition of the fractional flow function given in Appendix 1. The definition is meaningless if V is allowed to go to zero. In order to avoid this difficulty, V is set equal to some arbitrarily small positive number. This permits a continued application of the fractional flow function concept. It follows that, after such time as V is set equal to this arbitrarily small value, the computation of V by the integral equation is no longer necessary.

This reduces the computational time for subsequent time steps considerably.

Figure 17 illustrates a new situation that arises when the saturation front reaches the water table. Those saturations along the trailing edge of the front continue to move as before. But, in addition to this, saturations within a certain range along the water table are also available to move. These are the saturations between the point at which the trailing edge of the front intersects the water table and S_{ar}. The displacements of these latter saturations are proportional to the slope of the appropriate fractional flow function curve. Since the water table is a surface across which no flow occurs, the appropriate F_w curve is that for which V equals zero. The general shape of this curve (with V set equal to some arbitrarily small value rather than zero for the reasons given above) is shown in (b) of Figure 17. The corresponding displacement of all saturations after some time interval is shown by the dashed profile in (c) of the figure. It is apparent here that the saturation is a multiple valued function of z within a certain depth range. However, this physically unacceptable situation can be made acceptable by employing a previously described technique. The objectionable portion of the profile is replaced by a front. The position of the front is determined by imposing a material balance, wherein the areas of the two-cross hatched sections in the figure are made to be equal. The resulting saturation

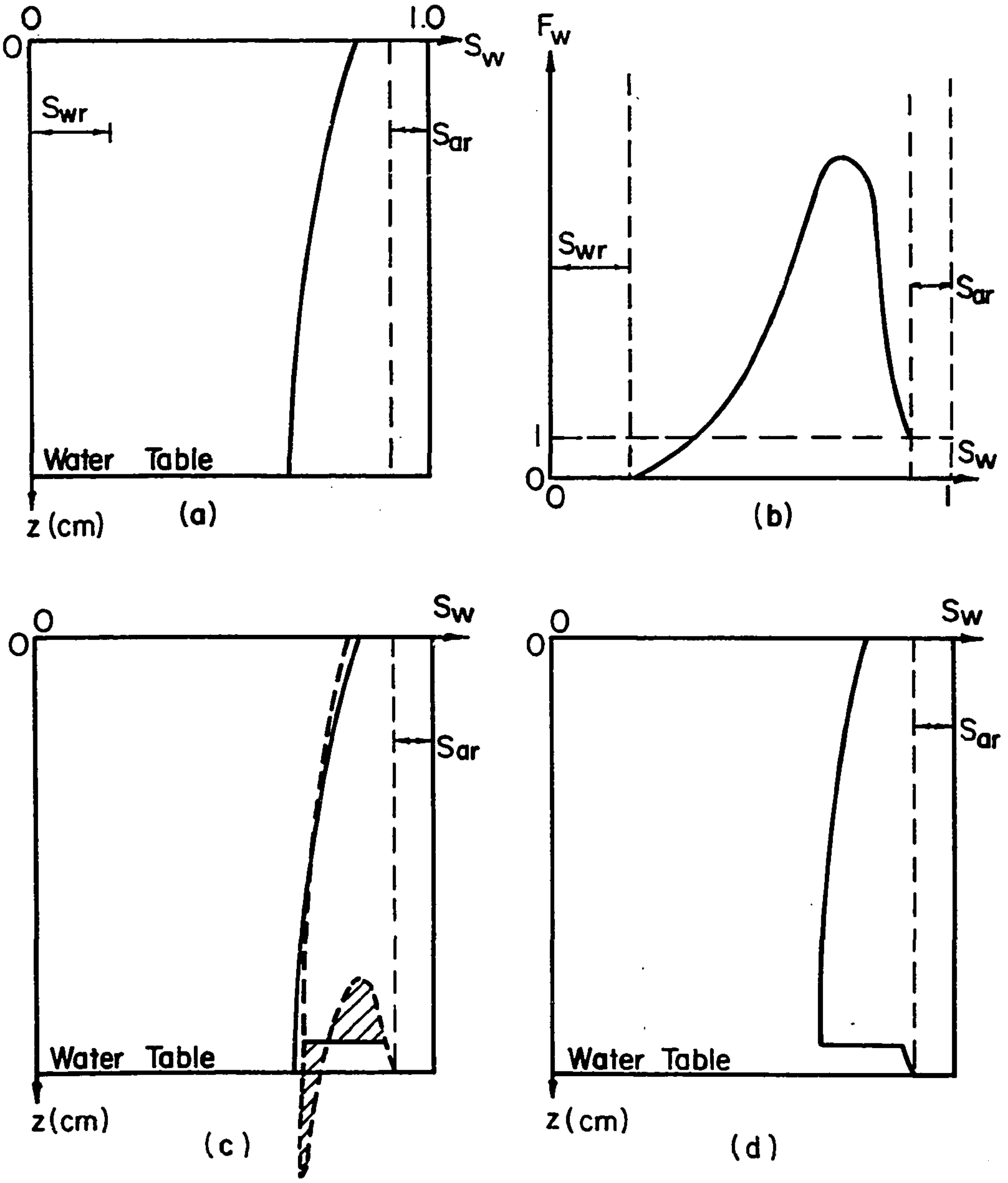

Fig. 17 The Developement of an Upward Moving Front.

profile is shown in (d) of Figure 17. Subsequent profiles are determined in a similar fashion.

The results of a computer analysis of the Case (2) problem are plotted in the next three figures. The progress of the saturation profile in the soil is traced in Figures 18 and 19. The profile is shown at an early stage of infiltration in (a) of Figure 18. Counterflow of air has not yet begun. However, the increased pressure in the air entrapped ahead of the front has already reduced the infiltration to a rate lower than that which existed in the semi-infinite medium at a corresponding time. In (b) of the figure it can be seen that the saturation at the surface has decreased below S_{ar}, as a result of counterflow, after only 0.110 hours. The early commencement of counterflow is a result of the pressure build up in the air ahead of the front. The rapid development of air counterflow is evident from a comparison of (b) and (c). After 0.393 hours, the total velocity has reached zero, and the air is exiting the soil at the same rate at which water is entering. Stages (d), (e), and (f) show the continued progress of the saturation front up to the time the front reaches the water table. During this period, the profile stretches but does not change its shape appreciably. In (g) an upward moving front is formed as the downward moving front is "reflected" from the water table. In (h) the soil is shown as it nears saturation.

The series of illustrations in Figures 18 and 19 demonstrate the extent to which the saturation profile may

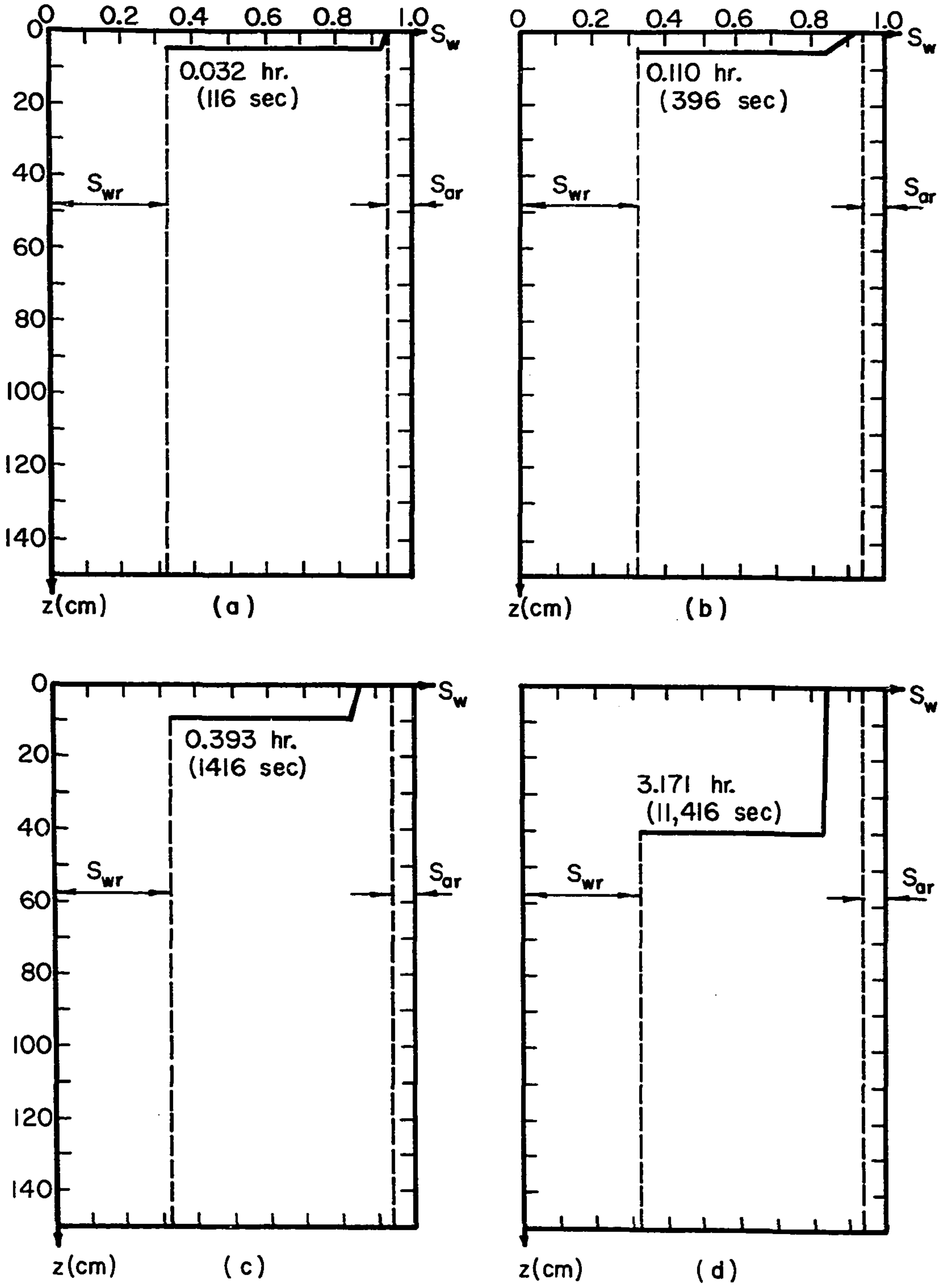

Figure 18 Progress of the Saturation Profile with Time (Water Table at a Depth of 150 cm. — Medium Characteristics as Shown in Figures 32 and 33 of Appendix 2)

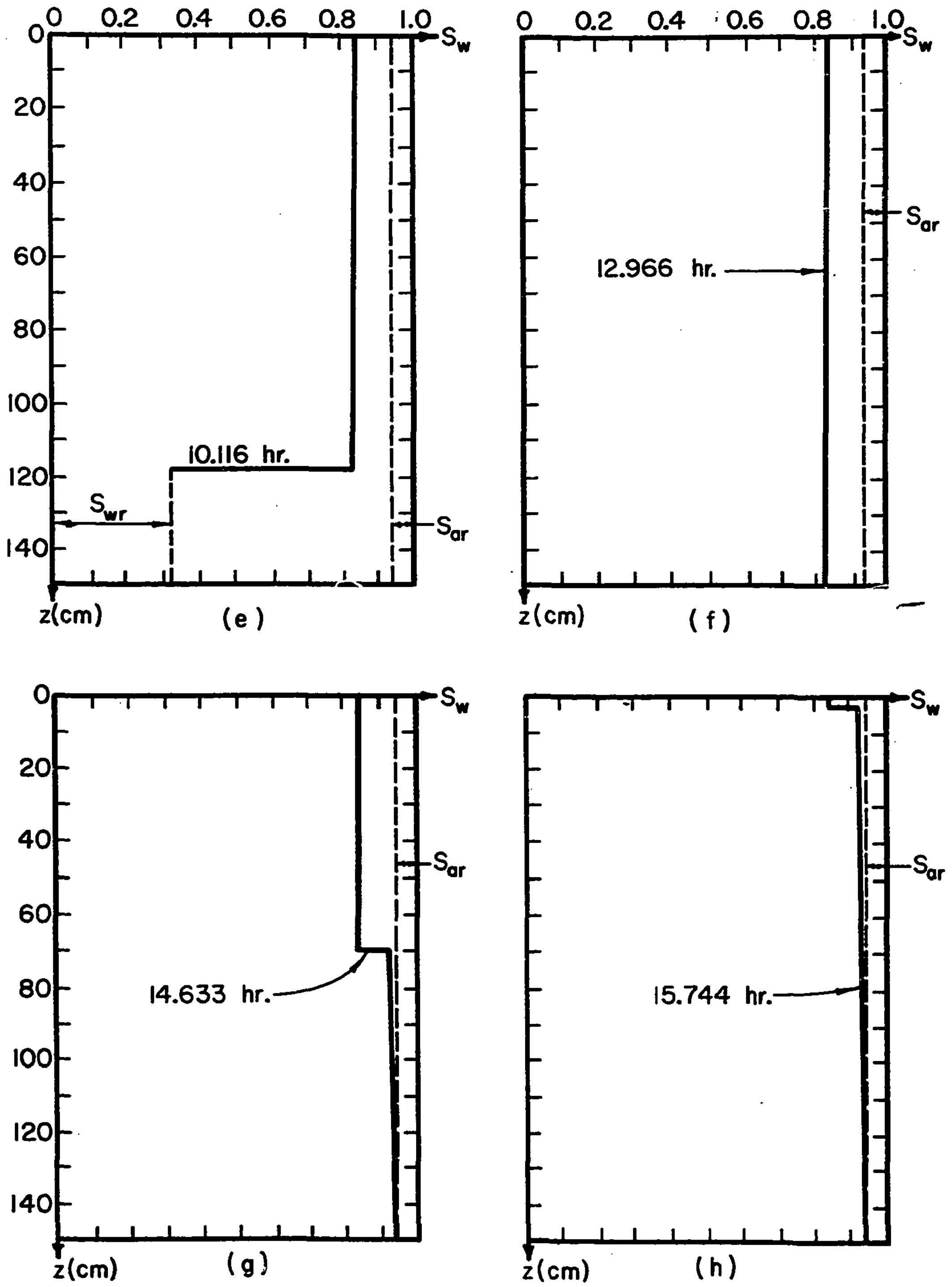

Figure 19 Progress of the Saturation Profile with Time
(Continuation of Figure 18)

be affected when air is not free to escape from the soil. It is primarily a matter of timing. When compared to the semi-infinite case, it is observed that the front advances much more slowly and that the shifting of the profile to allow for counterflow occurs much more rapidly.

The variation with time of the infiltration rate and the cumulative infiltration are shown in Figure 20. As in the semi-infinite medium, the infiltration rate is very high when infiltration begins because of the high capillary pressure gradient initially present. However, the infiltration rate decreases from this high value much more rapidly than in the case of the semi-infinite medium. This is to be expected, since, as was previously pointed out, the saturation profile moves more slowly when the added effect of air pressure build up is present. The infiltration rate actually decreases to a minimum value and then increases again. This result is physically reasonable in view of the changes that occur in the magnitudes of the important infiltration driving forces before and during the development of air counterflow. As water moves into the soil and increases the length of the wetted column, the gravity driving force increases. However, prior to counterflow, the simultaneously increasing pressure in the entrapped air provides a driving force which is opposite to the gravity force. Thus, before counterflow, the effect of the gravity force tends to be offset and infiltration is slowed. After counterflow of air has begun, and particularly after it is well developed, the

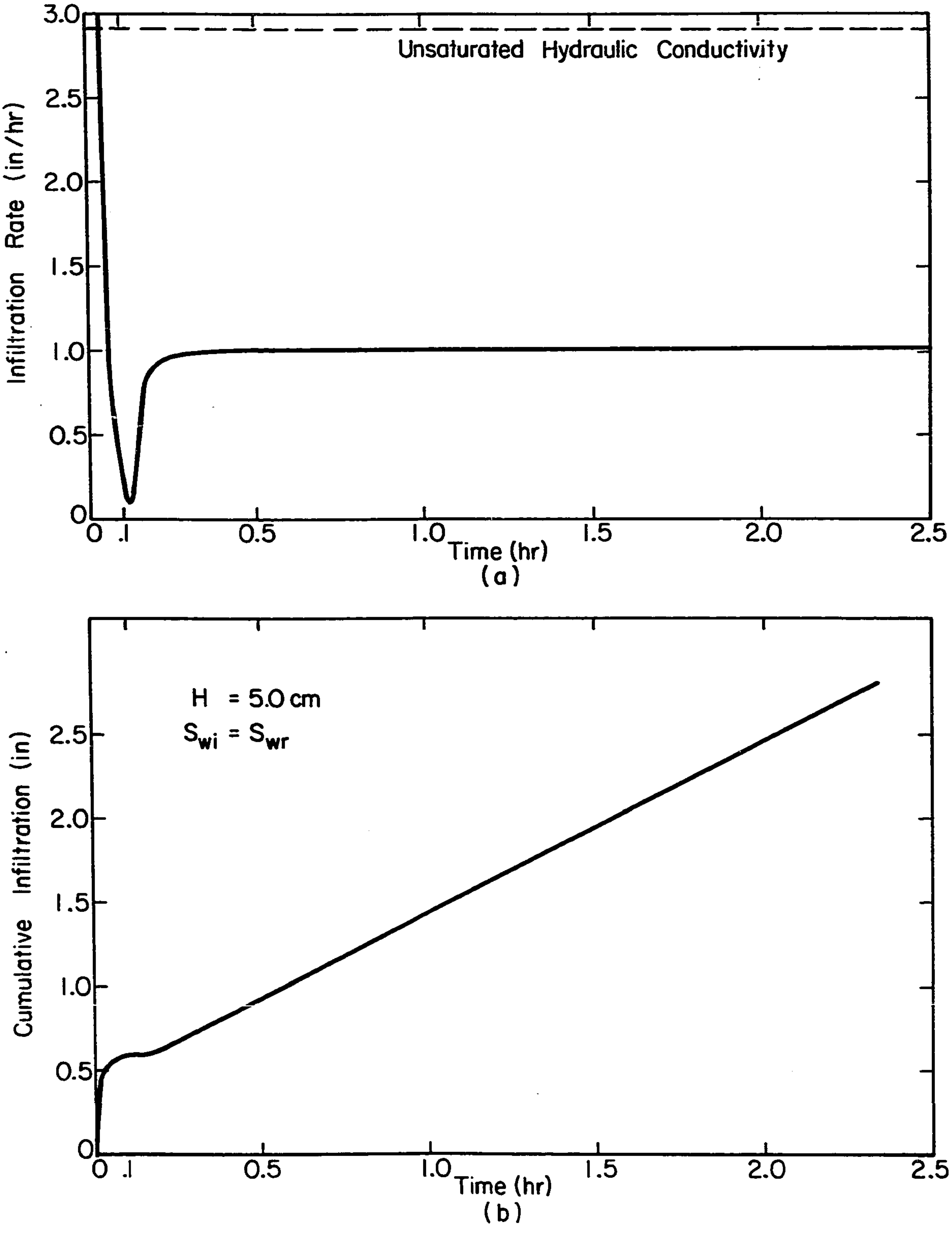

Figure 2.0 Infiltration Rate versus Time and Cumulative Infiltration versus Time. (Water Table at Depth of 150 cm — Medium Characteristics as Shown in Figures 32 and 33 of Appendix 2)

situation changes. The gravity force continues to increase as more water enters the soil, but the offsetting force, the compressive force, does not increase as rapidly as it did before counterflow. This is because some of the entrapped air is now able to escape by counterflowing. The result is a net increase in the downward driving force and an increased infiltration rate. Figure 20 shows that the increase in the infiltration rate is at first rapid, and then levels off and approaches a constant value. By the time the leveling off occurs, counterflow is well developed and the volume of air escaping from the medium is essentially equal to the volume of water entering the medium. The constant infiltration rate, which is approached, is less than the unsaturated hydraulic conductivity because air is counterflowing. It is also less than the constant rate approached in Case (1), because the retarding effect of air compression ahead of the front is now being considered. Figures 21 and 22 compare infiltration quantities for the Case (1) and (2) situations.

That an infiltration rate dip is predicted by the solution technique herein utilized, may be rather significant. Although the dip has been experimentally observed (28,29), the published results of other non-experimental solution methods makes no mention of such a dip. However, this is not surprising since these methods have generally not considered the added resistance due to the flow of air.

The significance of the infiltration rate dip in terms of the cumulative amount of water that has infiltrated is shown to be small in (b) of Figure 20.

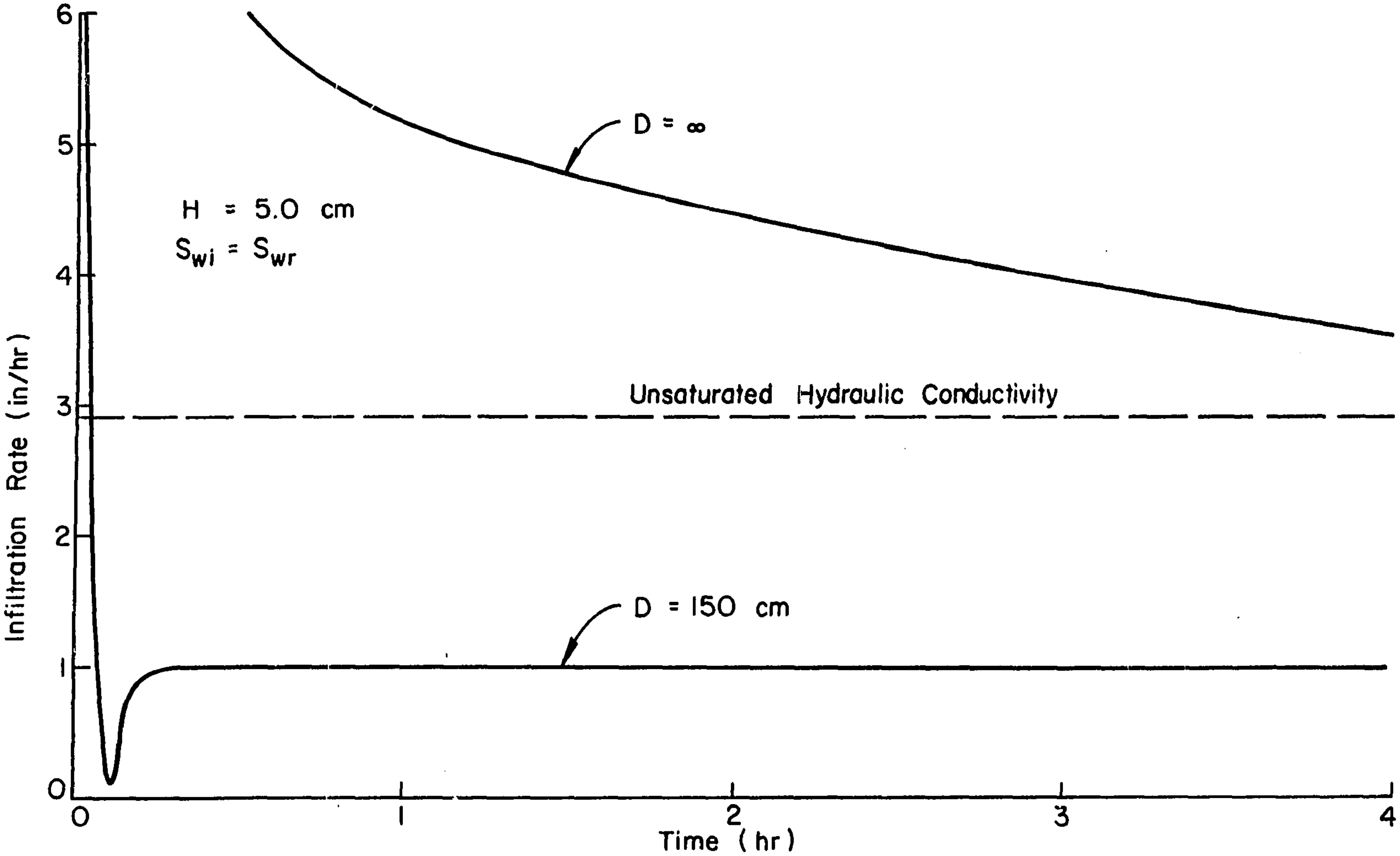

Figure 21 A Comparison of Infiltration Rates for a Finite Depth and an Infinite Depth Medium (Medium Characteristics are Shown in Figures 32 and 33)

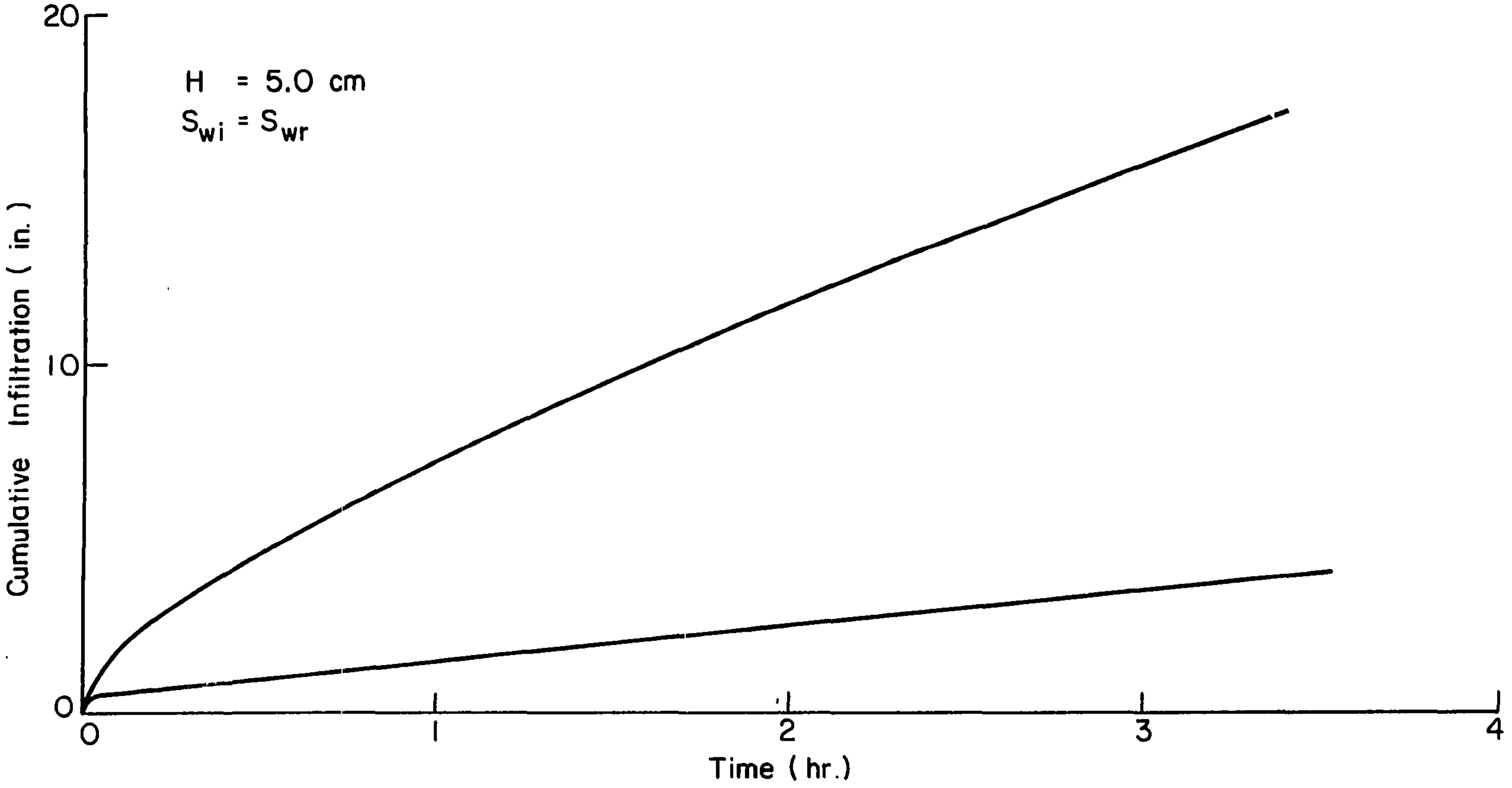

Figure 22 A Comparison of Cumulative Infiltration Quantities for a Finite Depth and an Infinite Depth Medium (Medium Characteristics are as Shown in Figures 32 and 33)

5.3 Case (3)

The boundary conditions remain unchanged from the previous case. Constant depth ponding is present at the upper boundary and a water table exists at the lower boundary. However, the initial water saturation, S_{wi}, is not considered to be equal to the residual water saturation, S_{wr}, as was previously supposed. It is now assumed that the initial water saturation is greater than the residual water saturation and uniform.

In the previous two cases, the water, which initially occupied the medium, was not able to move because the medium exhibits zero permeability to those water saturations at or below the residual water saturation. The medium is not, however, impermeable to initial water saturations which are greater than S_{wr}. This behavior is evident from a consideration of Figure 1. Consequently, in this third situation, the movement of that mobile water, which is initially present, must be considered.

Recalling that saturation displacements are proportional to the slope of the fractional flow function curve, the saturation profile would be expected to take on a shape similar to that in (a) of Figure 23, as infiltration begins. The saturation is seen to be a multiple valued function of z, both near the surface and near the water table. As before, the upper region of the profile can be made single valued by employing a construction of the Buckley-Leverett type on the appropriate fractional flow function curve. The

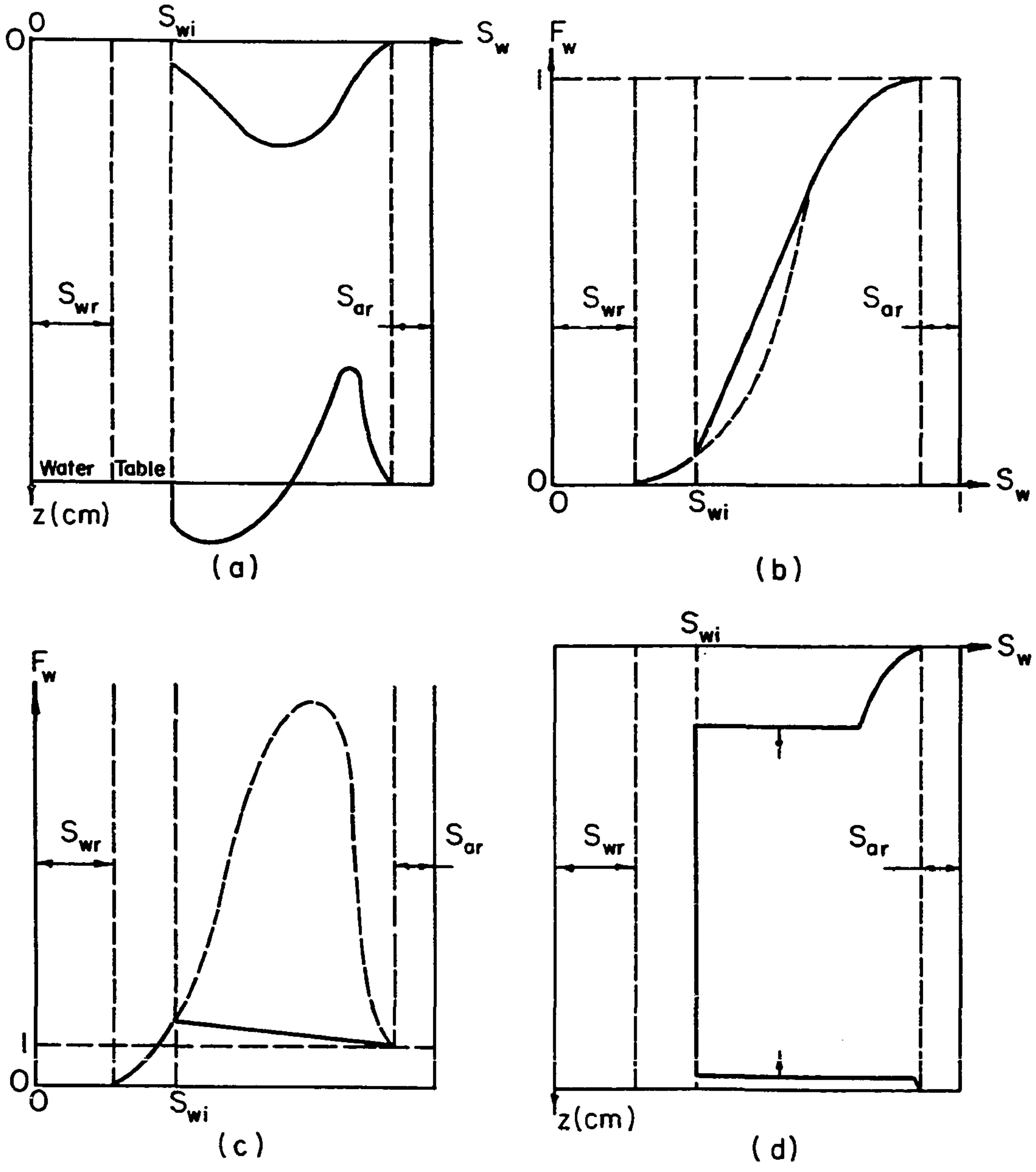

Figure 23 The Development of a Saturation Profile when $S_{wi} > S_{wr}$

appropriate curve and construction are illustrated in (b) of Figure 23. It should be noted that the secant now originates from S_{wi}, rather than S_{wr}. This is proper because the initial saturation is now S_{wi} and not S_{wr} The modification of the profile resulting from this construction is shown in the upper portion of (d) of Figure 23. The saturation profile near the water table is made single valued by the type of construction illustrated in (c) of the same figure. Here the appropriate F_w curve is that for which the total velocity is zero, since no flow occurs across the water table boundary. The secant originates at S_{wi} and is drawn tangent to the F_w curve. The velocities of all saturations between S_{wi} and the point of tangency are the same since each of these velocities is proportional to the slope of the secant. The modified profile takes on a form like that shown in the lower portion of (d) in Figure 23. Thus, when $S_{wi} > S_{wr}$, the profile consists of an upward moving front and a downward moving front. The cumulative infiltration at any time is proportional to the sum of the areas behind these two fronts. After the fronts meet, subsequent profiles may be determined in exactly the same way that they were determined after the downward moving front reached the water table in Case (2).

The results of a computer treatment of the Case (3) problem are illustrated in the next two figures. Figure 24 shows the development and progress of the saturation

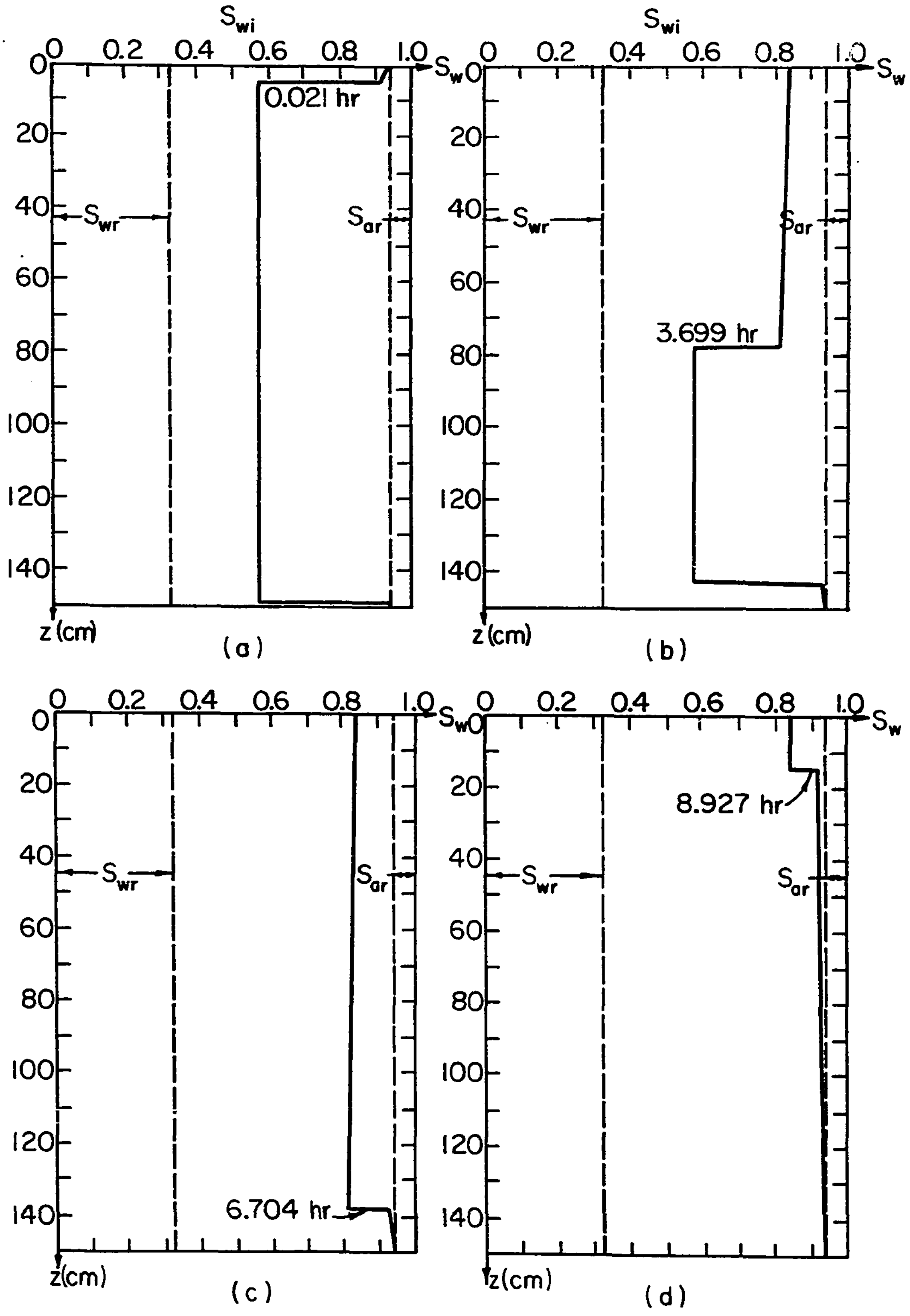

Figure 24 Progress of the Saturation Profile with Time (S_{wi}=0.575 — Medium Characteristics are Shown in Figures 32 and 33 of Appendix 2)

profile with time. An early stage of infiltration is represented in (a) of this figure. The two fronts have just started to advance toward each other and the pressure in the entrapped air has not yet increased sufficiently to cause air counterflow. In (b), a later stage, it can be seen that counterflow is already will developed, as indicated by the reduced saturation near the surface. This type of profile is typical until such time as the downward and upward moving fronts meet. The shape of the profile immediately after the two fronts have met is shown in (c) of the figure. The medium is almost fully saturated in (d).

In Figure 25, it can be seen that the infiltration rate curve and cumulative infiltration curve have the same general shape as was evidenced in Case (2). However, the position of the curves are shifted slightly in time. In the current situation, where $S_{wi} > S_{wr}$, the infiltration rate decreases more rapidly from its high initial value. Counterflow of air and the dip in the infiltration rate occur at earlier times as well. This shifting in time can be attributed to the retarding effect of a more rapid pressure increase in the air ahead of the front. The more rapid pressure increase is to be expected since the initial volume of air present in the medium is less when $S_{wi} > S_{wr}$, than when $S_{wi} = S_{wr}$.

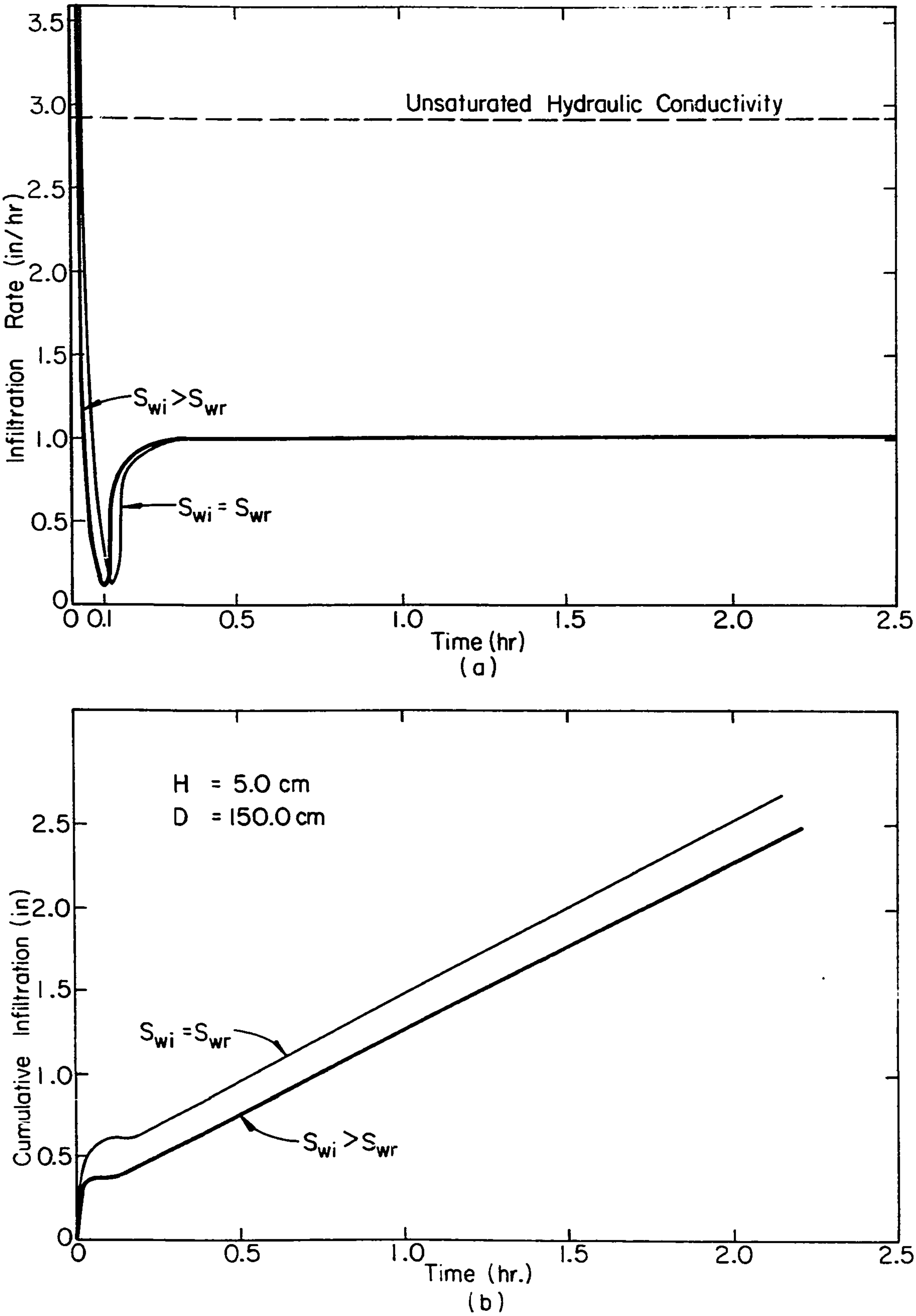

Figure 25 Infiltration versus Time and Cumulative Infiltration versus Time (Medium Characteristics are Shown in Figures 32 and 33)

5.4 Case (4)

In each of the previous cases, a certain set of soil-property relationships were specified. Boundary and initial conditions were also specified. Then, based on this input data, a solution to the infiltration problem was obtained. This solution is obviously dependent on the specified relationships and conditions - but to what extent? It is the purpose of this section to consider the extent of the dependency.

A qualitative indication of the sensitivity of the solution to changes in the input data is sought. This may be obtained by modifying that part of the input data, which is of interest (while keeping the other parts unchanged), and then observing the corresponding changes in the infiltration rate. The results of a number of applications of this procedure are illustrated in the next four figures.

Figure 26 shows the manner in which the infiltration rate is altered by changes in the boundary conditions. The effect of a variation in the depth of ponding at the surface, H, is illustrated in (a). The infiltration rate curve is shifted and distorted somewhat in time. However, the basic shape of the curve is unchanged and the same final rate is approached for each of the values of H considered. Part (b) of the figure demonstrates the effect of a variation in the water table depth, D. It is observed that the magnitude of the infiltration rate

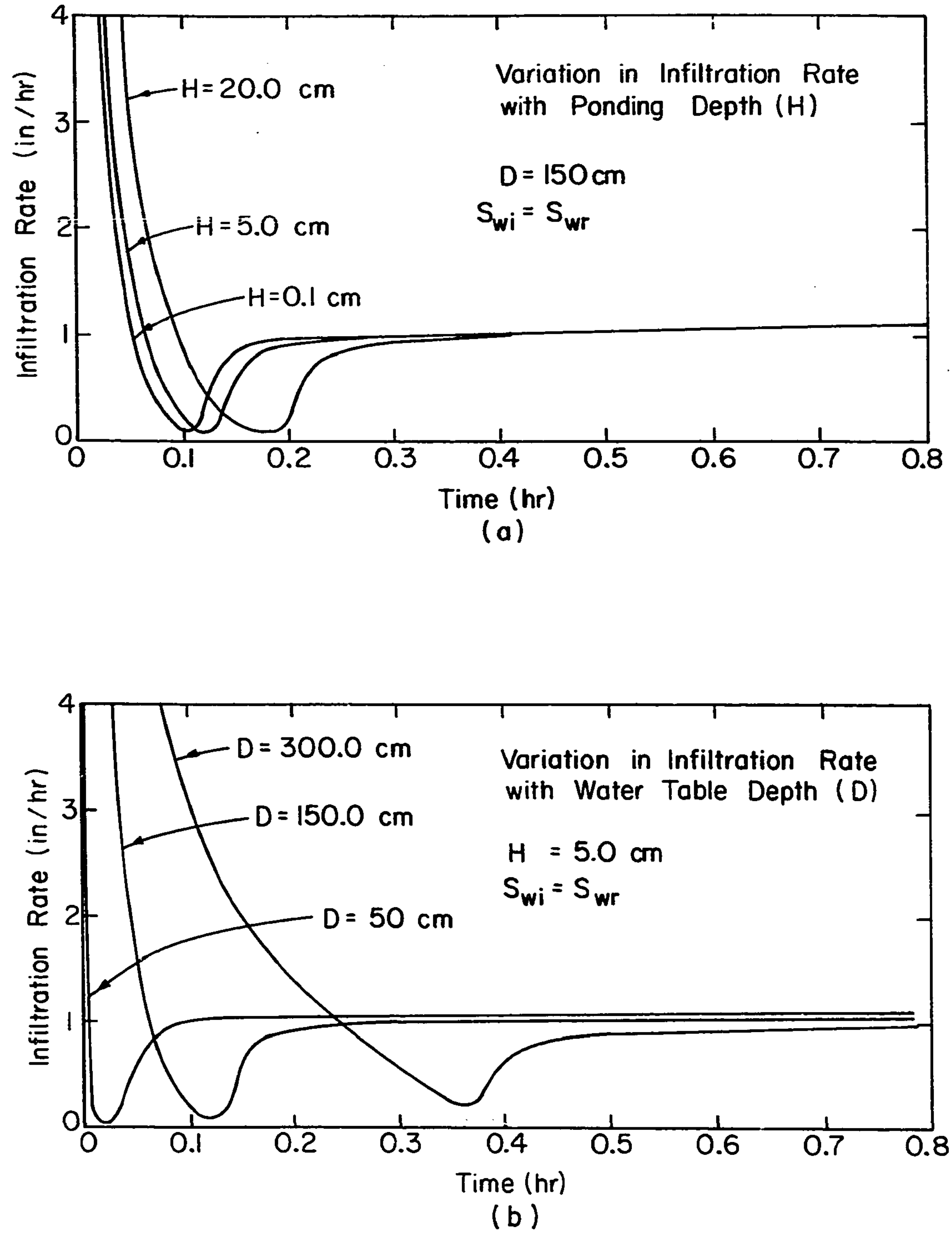

Fig 26 Variation in Infiltration Resulting from Changes in Boundary Conditions (Soil Properties are as Shown in Figures 32 and 33 of Appendix 2)

dip decreases with increasing D. This is consistent with the fact that no dip was present in the curve calculated for the semi-infinite medium in Case (1). It is also noted in (b) that the decrease in infiltration rate is more rapid when the water table depth is small. This is to be expected since a decreased water table depth results in a reduced initial air volume and, consequently, a more rapid pressure increase in the entrapped air as infiltration proceeds.

The effect on the infiltration rate of a change in the initial condition was previously touched upon in the Case (3) problem. An increase in the initial water saturation produced a change similar to that produced by the above mentioned decrease in water table depth.

An indication of the sensitivity of the infiltration problem solution to modifications in the basic soil-property relationships is provided by Figures 27, 28, and 29. In each of these figures, modified and unmodified soil-property relationships are presented along with the resulting infiltration rate curves. The modified relationships and corresponding infiltration rates are represented by the dashed lines. From Figures 27 and 28 it is evident that the final infiltration rates are highly dependent upon the forms of the relative permeability curves. It is also evident from Figure 28 that during the early stages of infiltration, the shape of the infiltration rate curve is quite sensitive to changes in the shape of the k_{ra}

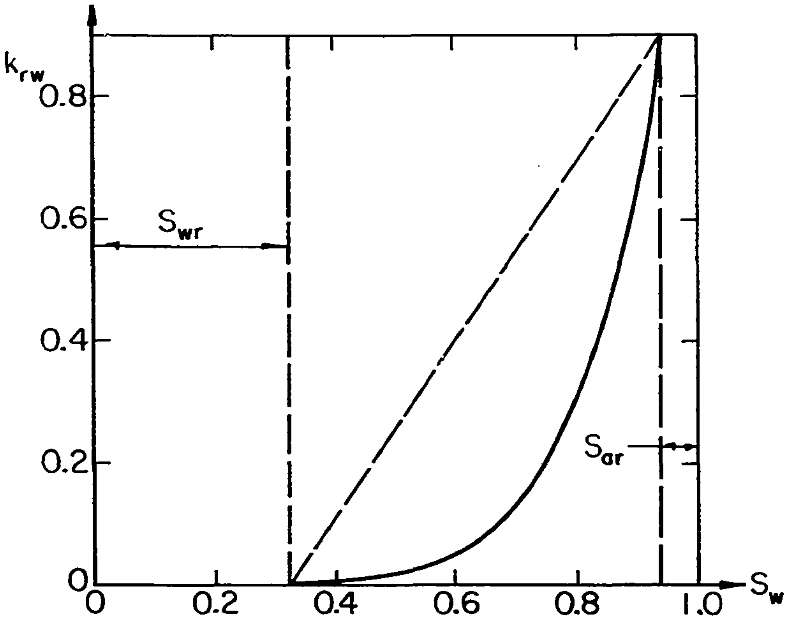

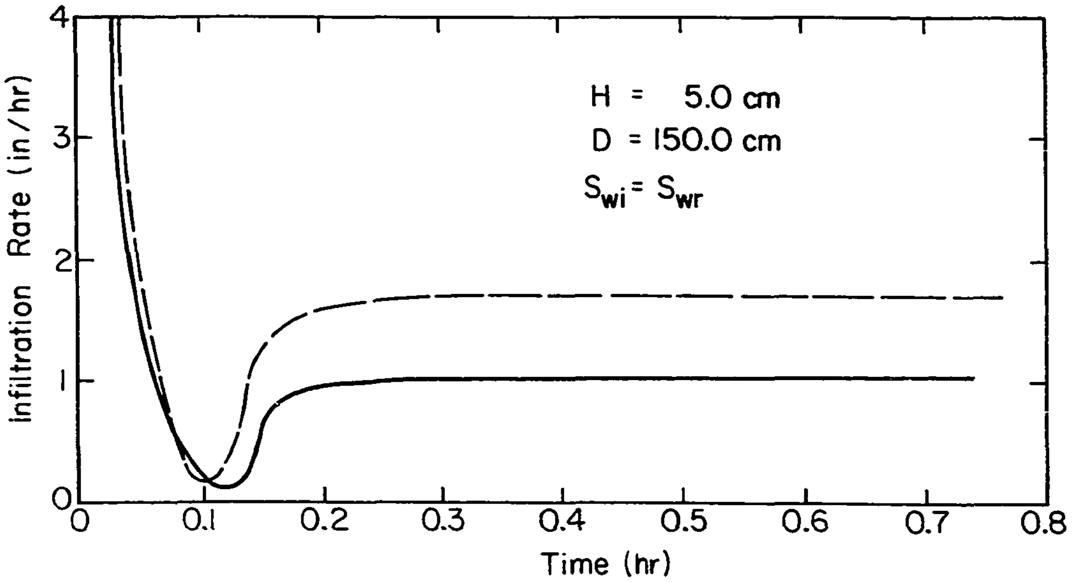

Figure 27 Variation in Infiltration Rate Resulting from a Change in the Relationship Between Water Saturation and Relative Permeability to Water (Other Soil Properties are as Shown in Figures 32 and 33 of Appendix 2)

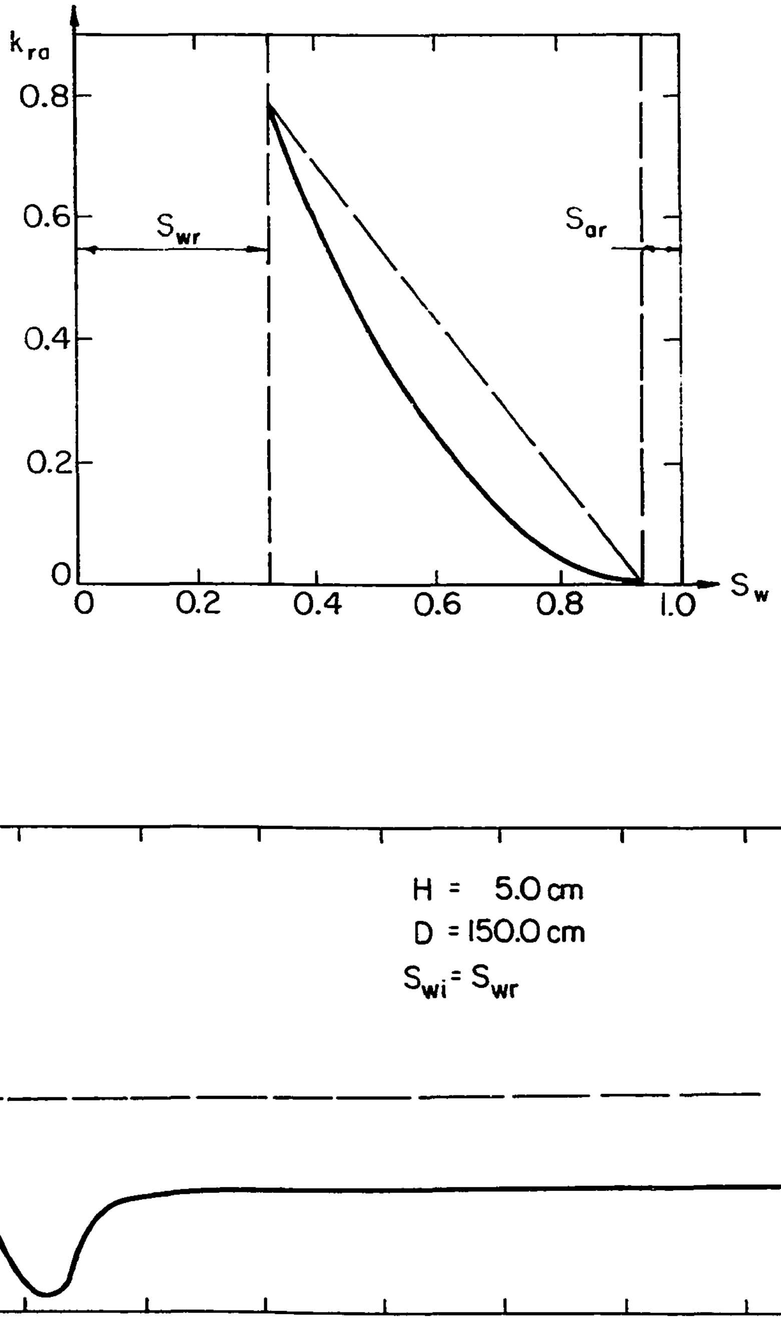

Fig 28 Variation in Infiltration Rate Resulting from a Change in the Relationship Between Water Saturation and Relative Permeability to Air. (Other Soil Properties are as Shown in Figures 32 and 33 of Appendix 2.)

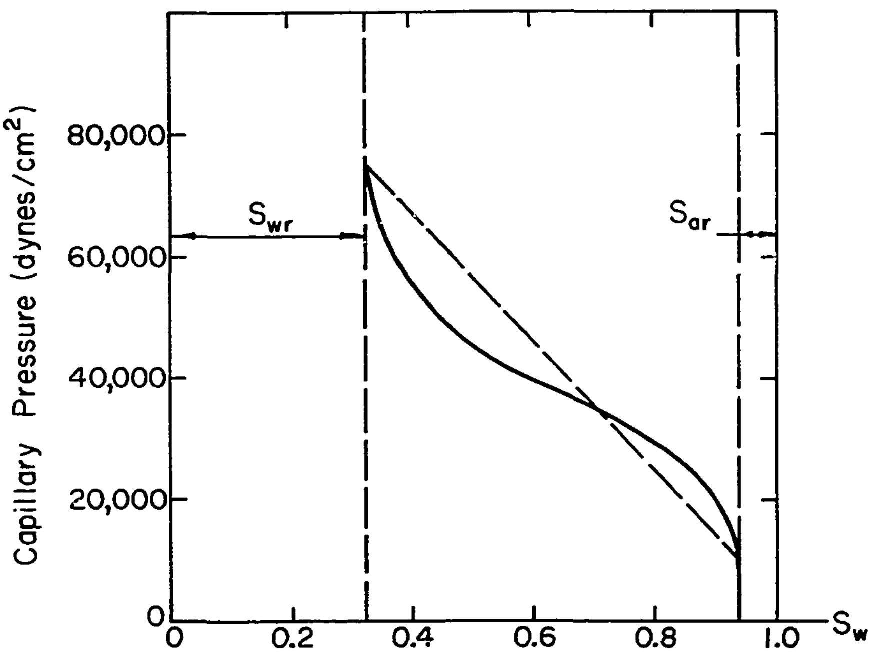

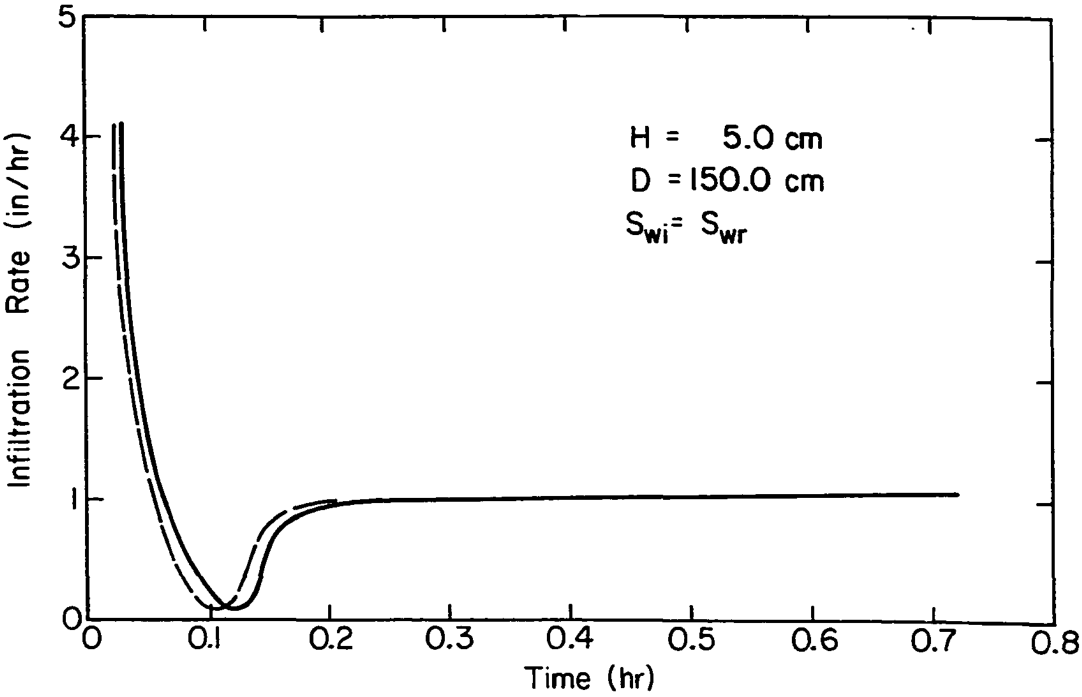

Figure 29 Variation in Infiltration Rate Resulting from a Change in the Relationship Between Water Saturation and Capillary Pressure. (Other Soil Properties are as Shown in Figures 32 and 33 of Appendix 2.)

versus S_w curve. The dip is almost non-existant when k_{ra} versus S_w is approximated by a straight line. This is not surprising in view of the large differences in k_{ra} values at saturations only slightly below S_{ar}. Thus, when counterflow is just beginning and the saturation at the surface is only slightly less than S_{ar}, the airflow will be less restricted in the modified soil due to its higher relative permeability to air. Consequently, the air pressure in the soil will build less rapidly, allowing the infiltration rate to remain at a higher level. The effect of a change in the capillary pressure versus saturation relationship is illustrated in Figure 29. The infiltration rate is seen to be less sensitive to changes in this relationship.

5.5 Case (5)

In this last section, an attempt is made to compare the results obtained from this investigation with results obtained, or obtainable, from other investigations.

The first comparision makes use of a finite difference solution scheme devised by Le Van Phuc (27). Necessary soil properties and boundary conditions are first assumed, and then analyses are performed using both the Buckley-Leverett and the finite difference approaches. The assumed soil properties, which were taken from Mr. Phuc's thesis, are illustrated in Figures 34 and 35. The assumed boundary and initial conditions are those of constant-depth ponding at the surface, simi-infinite depth of medium, and uniform initial water saturation. Similar time intervals are used for both computational schemes. In the Buckley-Leverett solution, the initial saturation front is assumed to extend into the soil a distance equal to one-half the grid size utilized in the finite difference solution. The results obtained from the two analyses are shown in Figure 30. Infiltration rates are seen to be in reasonably good agreement.

The computer costs for the above analyses are markedly different. Even when a large grid size (8 cm.) is used in the finite difference solution, the cost is found to be ten times greater than that of a Buckley-Leverett solution. This cost difference would be further increased with any decrease in grid size.

The second attempt to compare infiltration results involves the findings of Free and Palmer (28). It previously has been stated that Free and Palmer observed a dip in the infiltration rate for infiltration into a finite depth medium. In their paper, the authors provide infiltration rate data for infiltration into a column of sand closed at the bottom, and also a column of sand open at the bottom. They also indicate the porosity and sieve size of the sand medium. From this limited soil data, and the infiltration data on the open column, an attempt was made to deduce the remaining soil properties. The deduced properties could then be analyzed using the Buckley-Leverett method for a finite depth medium. The results of this analysis could then be checked against the results of Free and Palmer for a closed column.

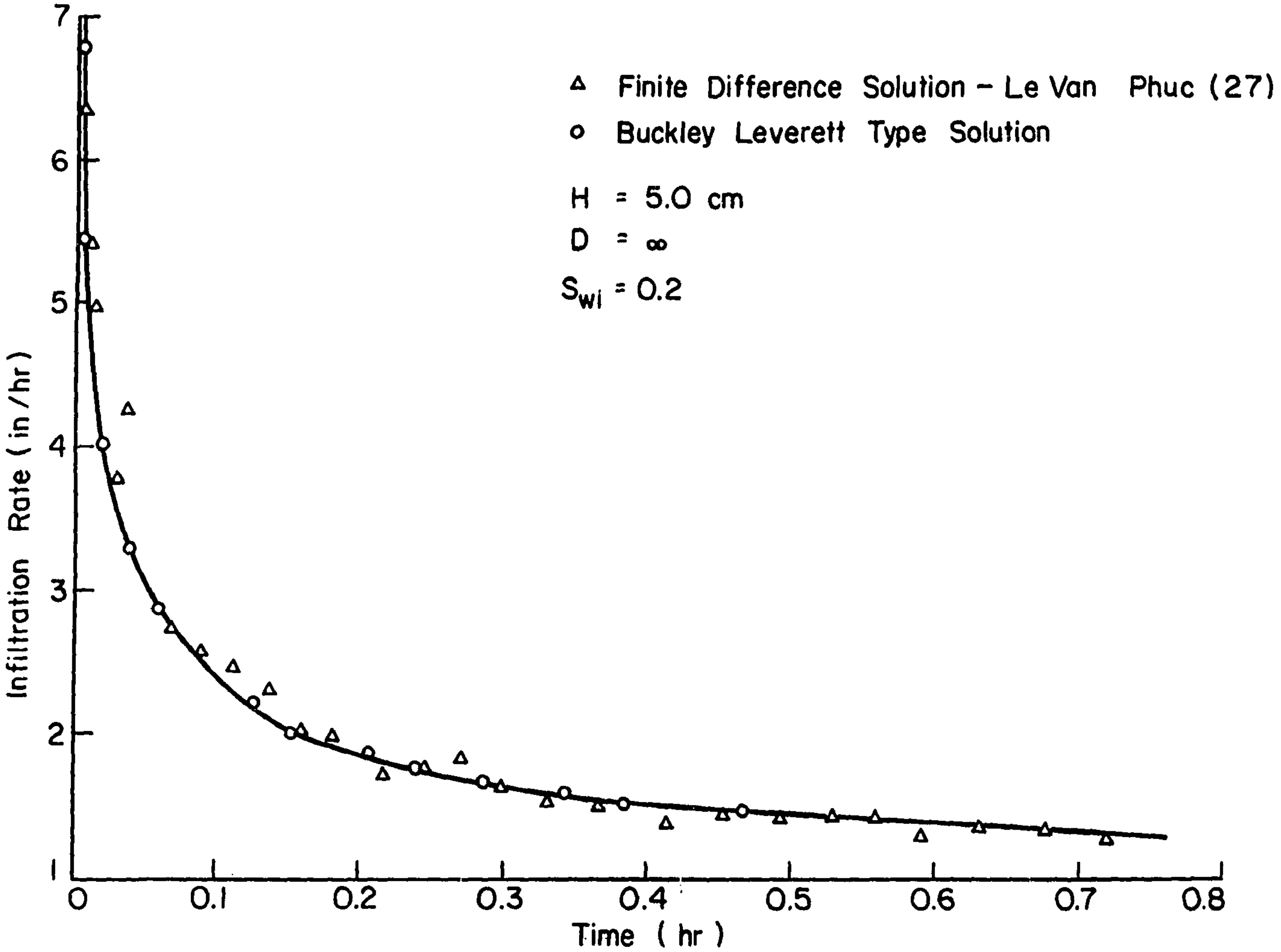

Figure 30 A Comparsion of Infiltration Rates as Obtained from a Finite Difference Solution and a Buckley-Leverett Type Solution

Numerous attempts to check the Buckley-Leverett results with those of Free and Palmer were unsuccessful. During the early stages of infiltration, the experimentally observed infiltration rates were consistantly higher than those obtained by the Buckley-Leverett solution. In addition, the counterflow of air and the dip in infiltration rate observed by Free and Palmer occurred at a much later time than did the counterflow and dip yielded by the Buckley-Leverett solution. The inability to check results is believed to be, in a large part, due to the fact that the data of Free and Palmer is for infiltration into an air-dry sand. This implies an initial water saturation which is considerably less than the residual water saturation, S_{wr}. Flow at saturations below S_{wr} is not governed by Darcy's law, and since the Buckley-Leverett approach is based on the validity of Darcy's law, its applicability is, at best, limited in this situation.

Although Free and Palmer do provide some information about infiltration into moist mediums, it is, unfortunately, not sufficiently detailed to permit a thorough comparision of results. The authors do note, however, that air counterflow occurred much more rapidly in moist mediums that in air-dry mediums. In one instance, they state that air counterflow was observed after only one minute in a moist sand, as compared to 160 minutes when the same sand was air dried. The moist mediums to which they refer were made moist by first allowing water to flow through them, and then allowing them to drain by gravity. The time of occurrence of counterflow, observed by Free and Palmer in mediums initially near residual saturation, is of the same order as that which is predicted by the Buckley-Leverett solution.

SUMMARY AND CONCLUSIONS

A new technique for the determination of infiltration rates has been presented in this paper. The technique has been employed to solve infiltration problems involving a variety of boundary, initial, and soil conditions. From all of this, a number of observations can be drawn that are of particular interest or significance:

1. The infiltration problem is a problem of two-phase flow in a porous medium. Thus, for a physically realistic treatment of the problem, the air phase must be given full consideration along with the water phase. The approach adopted in this study takes into account the resistance to air flow through the medium and the compressibility of air within the medium. These two phenomena, although known to influence infiltration rates (28, 29, 30), have been largely neglected by most previous non-experimental investigators.

2. Capillary pressure is partially neglected in the new technique. The principal effect of this partial neglect is to introduce inaccuracies into the shape of the saturation profile during the early stages of infiltration. However, these inaccuracies are acceptable for infiltration rate determinations since the infiltration rate is dependent upon the area under the saturation profile and not so much upon the shape of the saturation profile.

3. The technique herein employed has the advantage that, to a large degree, it is analytic. Numerical

procedures are employed only for integration and differentiation.

4. The technique yields results that prove to be in good qualitative agreement with published experimental results (28) -- even to the extent of predicting a dip in the infiltration rate in the case of the finite depth medium. The fact that the technique predicts this dip, when other solution schemes have not, appears to support the general validity of the approach.

5. Infiltration rate predictions yielded by the Buckley-Leverett type solution appear to be in reasonably good agreement with those predicted by a finite difference solution. This is quite promising in view of the fact that the computer costs are considerably less for a Buckley-Leverett type solution.

6. Infiltration rate determinations are sensitive to variations in some of the soil property relationships. This would indicate a need for accurate soil property measurements.

BIBLIOGRAPHY

BIBLIOGRAPHY

1. Buckley, S. E. and Leverett, M. C., "Mechanism of Fluid Displacement in Sands," Trans. A.I.M.E., Vol. 146, pp. 107-116, 1942.

2. Buckingham, Edgar, "Studies on the Movement of Soil Moisture," U.S. Dept. Agr. Bur. Soils Bull. 38, 1907.

3. Green, W. H. and Ampt, G. A., "Studies on Soil Physics: 1. The Flow of Air and Water Through Soils," J. Agr. Sci., Vol. IV, pp. 1-24, 1911.

4. Gardner, W. and Widstoe, J. A., "The Movement of Soil Moisture," Soil Sci., Vol. 11, pp. 215-232, 1921.

5. Kostiakov, A. N., "On the Dynamics of the Coefficient of Water-Percolation in Soils and the Necessity of Studying It From a Dynamic Point of View for Purposes of Amelioration," Trans. 6th Comm. Intern. Soil Sci. Soc. Russian Part A, pp. 17-21, 1932.

6. Horton, R. E., "An Approach Toward Physical Interpretation of Infiltration Capacity," Soil Sci. Soc. of Amer. Proc., Vol. 5, pp. 399-417, 1940.

7. Holtan, H. N., "A Concept for Infiltration Estimates in Watershed Engineering," U.S. Dept. Agr., A.R.S. Pub., pp. 41-51, 1961.

8. Richards, L. A., "Capillary Conduction of Liquids Through Porous Mediums," Physics, Vol. 1, pp. 318-333, 1931.

9. Childs, E. C., "The Transport of Water Through Heavy Clay Soils," J. Agr. Sci., Vol. 26, pp. 527-545, 1936.

10. Childs, E. C. and Collis-George, N., "The Permeability of Porous Materials," Proc. Roy. Soc. London, Series A, Vol. 201, No. 1066, pp. 392-405, 1950.

11. Klute, A., "A Numerical Method for Solving the Flow Equation For Water in Unsaturated Materials," Soil Sci., Vol. 73, pp. 105-116, 1952.

12. Crank, J. and Henry, M. E., "Diffusion in Media with Variable Properties, I & II," Trans. Faraday Soc., Vol. 45, pp. 636-642, 1119-1128, 1949.

13. Philip, J. R., "The Theory of Infiltration: 1. The Infiltration Equation and Its Solution," Soil Sci., Vol. 83, pp. 345-357, 1957.

14. Philip, J. R., "The Theory of Infiltration: 2. The Profile of Infinity," Soil Sci., Vol. 83, pp. 435-448, 1957.

15. Philip, J. R., "The Theory of Infiltration: 3. Moisture Profiles and Relation to Experiment," Soil Sci., Vol. 84, pp. 97-182, 1957.

16. Philip, J. R., "The Theory of Infiltration: 4. Sorptivity and Algebraic Infiltration Equation," Soil Sci., Vol. 84, pp. 257-264, 1957.

17. Philip, J. R., "The Theory of Infiltration: 5. The Influence of Initial Moisture Content," Soil Sci., Vol. 84, pp. 329-339, 1957.

18. Hanks, R. J. and Bowers, S. A., "Numerical Solution of the Moisture Flow Equation for Infiltration into Layered Soils," Soil Sci. Soc. of Amer. Proc., Vol. 26, No. 6, pp. 530-534, 1962.

19. Rubin, J. and Steinhardt, R., "Soil Water Relations during Rain Infiltration: 1. Theory," Soil Sci. Soc. of Amer. Proc., Vol. 27, No. 3, pp. 246-251, 1963.

20. Whisler, F. D. and Klute, A., "The Numerical Analysis of Infiltration, Considering Hysteresis, into a Vertical Soil Column at Equilibrium under Gravity," Soil Sci. Soc. of Amer. Proc., Vol. 29, No. 5, pp. 489-494, 1965.

21. Ibrahim, H. A., "Hysteresis and Intermittent Vertical Infiltration in Unsaturated Porous Media," Ph.D. Thesis, Cornell University, 1967.

22. Freeze, R. A., "The Mechanism of Natural Ground Water Recharge and Discharge: 1. One-Dimensional, Vertical, Unsteady, Unsaturated Flow above a Recharging or Discharging Ground-Water Flow System," Water Resources Research, Vol. 5, No. 1, pp. 153-171, 1969.

23. Welge, H. J., "A Simplified Method for Computing Oil Recovery by Gas or Water Drive," Trans. A.I.M.E., Vol. 195, pp. 91-98, 1952.

24. Martin, J. C., "The Theory of One-Dimensional Two-Phase Flows of Incompressible Fluids," Producers Monthly, Vol. 24, No. 9, pp. 18-29, 1960.

25. Morel-Seytoux, H. J., "Flow of Immiscible Fluids in Porous Media: Part 1. and Part 2.," Unpublished Report for Chevron Research, pp. 1-433.

26. Brooks, R. H., "Hydraulic Properties of Porous Media," Ph.D. Thesis, Colorado State University, Fort Collins, Colorado, 1965.

27. Phuc, Le Van, "General One-dimensional Model for Infiltration," M. S. Thesis, Colorado State University, Fort Collins, Colorado, 1969.

28. Free, J. R., and Palmer, V. J., "Relationship of Infiltration, Air Movement, and Pore Size in Graded Silica Sand," Soil Sci. Soc. of Amer. Proc., Vol. 5, pp. 390-398, 1940.

29. Peck, A. J., "Moisture Profile Development and Air Compression During Water Uptake by Bounded Porous Bodies: 3. Vertical Columns," Soil Sci., Vol. 100, No. 1, pp. 44-51, 1964.

30. Adrian, D. D., and Franzini, J. B., "Impedance to Infiltration by Pressure Build-Up Ahead of the Wetting Front," J. Geophys. Res., Vol. 71, No. 4, pp. 5857-5863, 1966.

31. Sheidegger, A. E., "The Physics of Flow Through Porous Media," University of Toronto Press, relevant pages: 74, 216, 1960.

32. Pirson, S. J., "Oil Reservoir Engineering," McGraw Hill Book Company, Inc., relevant page: 437.

33. Smail, L. L., "Calculus," Appleton-Century-Crofts, Inc., relevant page: 131, 1949.

APPENDIX 1

MATHEMATICAL DEVELOPMENTS

Appendix 1

MATHEMATICAL DEVELOPMENTS

Development of an Expression for the Fractional Flow Function

The vertical coordinate z is taken as positive in the downward direction throughout this study.

For flow in the vertical direction, Darcy's law generalized (31) to multi-phase (32) flow may be written in the differential form:

$$V_w = - \frac{k\,k_{rw}}{\mu_w}\left[\frac{\partial p_w}{\partial z} - \rho_w g\right] \qquad \text{(A1)}$$

for the water phase, and

$$V_a = - \frac{k\,k_{ra}}{\mu_a}\left[\frac{\partial p_a}{\partial z} - \rho_a g\right] \qquad \text{(A2)}$$

for the air phase, where V is the velocity, k is the intrinsic permeability, k_{ri} is the relative permeability of phase i, μ is the viscosity, p is the pressure, ρ is the density, g is the acceleration of gravity, and z is the vertical coordinate.

Since air and water are immiscible fluids there exists a pressure difference between the two fluids, which is the capillary pressure p_c:

$$p_c(S_w) = p_a - p_w \qquad \text{(A3)}$$

The capillary pressure is a function of the water saturation, S_w.

The fractional flow function is defined as

$$FW = \frac{V_w}{V_a + V_w}$$

A more useful form of the fractional flow function can be obtained by combining this definition with the three previous equations. It will be convenient to let

$$\lambda_a = \frac{k\,k_{ra}}{\mu_a} \quad \text{and} \quad \lambda_w = \frac{k\,k_{rw}}{\mu_w}$$

Multiplying equation (A1) by λ_a and equation (A2) by λ_w and then subtracting equation (A2) from equation (A1) yields

$$V_w\lambda_a - V_a\lambda_w = \lambda_w\lambda_a\left[\frac{\partial}{\partial z}(p_a - p_w)\right] + \lambda_w\lambda_a g(\rho_w - \rho_a)$$

Now according to equation (A3), this may be written as

$$V_w\lambda_a - V_a\lambda_w = \lambda_w\lambda_a \frac{\partial p_c}{\partial z} + \lambda_w\lambda_a g(\rho_w - \rho_a)$$

If the difference in densities is defined as

$$\Delta\rho = \rho_w - \rho_a$$

the equation becomes

$$V_w\lambda_a - V_a\lambda_w = \lambda_w\lambda_a \frac{\partial p_c}{\partial z} + \lambda_w\lambda_a g\Delta\rho \qquad \text{(A4)}$$

Now define a total velocity (algebraic velocity) to be

$$V = V_a + V_w$$

Substituting for V_a in equation (A4) yields

$$V_w\lambda_a - \lambda_w(V-V_w) = \lambda_w\lambda_a \frac{\partial p_c}{\partial z} + \lambda_w\lambda_a g\Delta\rho$$

or

$$V_w(\lambda_a + \lambda_w) = V\lambda_w + \lambda_w\lambda_a \frac{\partial p_c}{\partial z} + \lambda_w\lambda_a g\Delta\rho$$

Dividing by $(\lambda_a + \lambda_w)$,

$$V_w = \frac{\lambda_w}{\lambda_a + \lambda_w}\left[V + \lambda_a \frac{\partial p_c}{\partial z} + \lambda_a g\Delta\rho\right]$$

Substituting this equation into the definition of the fractional flow function gives

$$FW = \frac{V_w}{V_w + V_a} = \frac{V_w}{V} = \frac{\lambda_w}{\lambda_a + \lambda_w}\left[1 + \frac{\lambda_a}{V}\left(\frac{\partial p_c}{\partial z} + \Delta\rho g\right)\right]$$

Now let

$$f_w = \frac{\lambda_w}{\lambda_a + \lambda_w} = \frac{\dfrac{k\,k_{rw}}{\mu_w}}{\dfrac{k\,k_{ra}}{\mu_a} + \dfrac{k\,k_{rw}}{\mu_w}} = \frac{1}{1 + \dfrac{k_{ra}}{\mu_a}\dfrac{\mu_w}{k_{rw}}}$$

and the resulting equation may be written

$$FW = f_w\left[1 + \frac{k\,k_{ra}}{\mu_a V}\left(\frac{\partial p_c}{\partial z} + \Delta\rho g\right)\right]$$

This equation represents the fractional flow function in a general form. If the effects of both capillarity and gravity are neglected, a modified form of the fractional flow function results:

$$FW = f_w = \frac{1}{1 + \frac{k_{ra}}{\mu_a}\frac{\mu_w}{k_{rw}}}$$

If only the effect of capillarity is neglected, the modified form is

$$FW = F_w = f_w\left[1 + \frac{k\,k_{ra}}{V\mu_a}\Delta\rho g\right]$$

Derivation of the Saturation Equation [equation (1) in text]

For flow in the z direction, the continuity equation for the water phase may be written

$$\phi\,\frac{\partial S_w}{\partial t} = -\,\frac{\partial V_w}{\partial z}$$

where the terms are as previously defined. And from a previous development, the fractional flow function is

$$FW = \frac{V_w}{V} = f_w\left[1 + \frac{k\,k_{ra}}{V\mu_a}\left(\frac{\partial p_c}{\partial z} + \Delta\rho g\right)\right]$$

Substituting for V_w in the continuity equation yields

$$\phi\,\frac{\partial S_w}{\partial t} = -\,\frac{\partial}{\partial z}\,V\left\{f_w\left[1 + \frac{k\,k_{ra}}{V\mu_a}\left(\frac{\partial p_c}{\partial z} + \Delta\rho g\right)\right]\right\} \qquad (A5)$$

and after rearranging, this equation becomes

$$\phi\,\frac{\partial S_w}{\partial t} = -\,\frac{\partial}{\partial z}\left(Vf_w + \frac{k\,k_{ra}}{\mu_a}f_w\Delta\rho g + \frac{k\,k_{ra}}{\mu_a}f_w\,\frac{\partial p_c}{\partial z}\right)$$

From the previous development of the fractional flow function it is known that

$$Vf_w + \frac{k\,k_{ra}}{\mu_a} f_w \Delta\rho g = V\left[f_w\left(1 + \frac{k\,k_{ra}}{V\mu_a}\Delta\rho g\right)\right] = VF_w$$

and, as a result, the previous equation can be expressed as

$$\phi \frac{\partial S_w}{\partial t} = -\frac{\partial}{\partial z}\left(VF_w + \frac{k\,k_{ra}}{\mu_a} f_w \frac{\partial p_c}{\partial z}\right)$$

Since the capillary pressure is a function of the water saturation, the equation can be written

$$\phi \frac{\partial S_w}{\partial t} = -\frac{\partial}{\partial z}\left(VF_w + \frac{k\,k_{ra}}{\mu_a} f_w \frac{dp_c}{dS_w}\frac{\partial S_w}{\partial z}\right)$$

This equation is a general form of the saturation equation.

Development of a Buckley-Leverett Type Equation [equation (2) in text]

As previously shown, a general form of the saturation equation may be written as

$$\phi \frac{\partial S_w}{\partial t} = -\frac{\partial}{\partial z}\left\{VF_w + \frac{k\,k_{ra}}{\mu_a} f_w \frac{dp_c}{dS_w}\frac{\partial S_w}{\partial z}\right\}$$

Now if it is assumed that the capillary pressure is negligible, the equation may be written in the much simpler form

$$\phi \frac{\partial S_w}{\partial t} = -\frac{\partial}{\partial z}\{VF_w\}$$

Because of the compressibility of air, the total velocity V may not be independent of z. However, if $\bar{V}$ is considered to be the average total velocity within the two-phase flow region, then V will be independent of z. And since F_w is a function of the water saturation S_w,

$$\phi \frac{\partial S_w}{\partial t} = - V \frac{\partial F_w}{\partial z} = - V \frac{dF_w}{dS_w} \frac{\partial S_w}{\partial z} \tag{B1}$$

As infiltration proceeds, the water saturation can be expected to vary with time and distance from the ground surface. This relationship can be expressed in a functional form as $S_w = S_w(z,t)$ or, equivalently, in a differential form as

$$dS_w = \frac{\partial S_w}{\partial z} dz + \frac{\partial S_w}{\partial t} dt$$

If the path of a single value of saturation is considered, the functional relationship becomes $S_w = S_w(z,t) = \text{constant}$, and the equivalent differential relationship becomes

$$0 = \frac{\partial S_w}{\partial z} dz + \frac{\partial S_w}{\partial t} dt \tag{B2}$$

Equations (B1) and (B2) may now be combined to give a Buckley-Leverett type of expression for the velocity of a saturation value, $\left(\frac{dz}{dt}\right)_{S_w}$. Eliminating $\frac{\partial S_w}{\partial z}$ from equations (B1) and (B2) yields

$$\left(\frac{dz}{dt}\right)_{S_w} = \frac{V}{\phi} \frac{dF_w}{dS_w} = \frac{V}{\phi} F'_w \tag{B3}$$

Development of an Integral Equation Relating Total Velocity to the Pressures at Two Positions [equation (4) in text]

For flow in the vertical direction Darcy's law may be written

$$V_w = -\lambda_w \left[\frac{\partial p_w}{\partial z} - \rho_w g\right]$$

for the water phase, and

$$V_a = -\lambda_a \left[\frac{\partial p_a}{\partial z} - \rho_a g\right]$$

for the air phase, where the terms are as previously defined. Adding these two equations and substituting for p_a, from the capillary pressure relationship, $p_c = p_a - p_w$, yields

$$V = -\lambda_w \left(\frac{\partial p_w}{\partial z} - \rho_w g\right) - \lambda_a \left(\frac{\partial p_c}{\partial z} + \frac{\partial p_w}{\partial z} - \rho_a g\right)$$

Rearranging and dividing by $(\lambda_w + \lambda_a)$ gives

$$\frac{V}{\lambda_w + \lambda_a} = -\frac{\partial p_w}{\partial z} - \frac{\lambda_a}{\lambda_w + \lambda_a}\frac{\partial p_c}{\partial z} + \frac{\lambda_w}{\lambda_w + \lambda_a}\rho_w g$$

$$+ \frac{\lambda_a}{\lambda_w + \lambda_a}\rho_a g \qquad \text{(C1)}$$

The quantity $\frac{\lambda_w}{\lambda_w + \lambda_a}$ has previously been defined as

$$f_w = \frac{\lambda_w}{\lambda_w + \lambda_a}$$

and the quantity $\frac{\lambda_a}{\lambda_w + \lambda_a}$ can similarly be defined as

$$f_a = \frac{\lambda_a}{\lambda_w + \lambda_a}$$

where $f_a + f_w = 1$. Substituting these relations into (C1) yields

$$\frac{V}{\lambda_w + \lambda_a} = -\frac{\partial p_w}{\partial z} - (1 - f_w)\frac{\partial p_c}{\partial z} + (1 - f_a)\rho_w g + f_a \rho_a g$$

which, upon simplification, gives

$$\frac{V}{\lambda_w + \lambda_a} = -\frac{\partial p_w}{\partial z} - (1 - f_w)\frac{\partial p_c}{\partial z} + \rho_w g - (1 - f_w) g(\rho_w - \rho_a)$$

Now at any fixed time t, the dependent variables are functions of z only, and the equation can be written

$$\frac{V}{\lambda_w + \lambda_a} = -\frac{dp_w}{dz} - (1 - f_w)\frac{dp_c}{dz} + \rho_w g - (1 - f_w) g(\rho_w - \rho_a)$$

Integrating with respect to z, rearranging, and recalling the definition of λ_w and λ_a, yields

$$-\int_1^2 dp_w + \int_1^2 \rho_w g dz = V\int_1^2 \frac{dz}{k\left(\frac{k_{ra}}{\mu_a} + \frac{k_{rw}}{\mu_w}\right)}$$

$$+ g(\rho_w - \rho_a)\int_1^2 (1 - f_w) dz + \int_1^2 (1 - f_w) dp_c$$

This expression relates the average total velocity, V, to the pressures at positions 1 and 2.

Prove that any Straight Line Approximation to the F_w Curve Results in a Material Balance on the Corresponding Saturation Profile

An arbitrary secant construction b'-c' is shown on the F_w curve in Figure 31, along with the corresponding front on the F'_w curve.

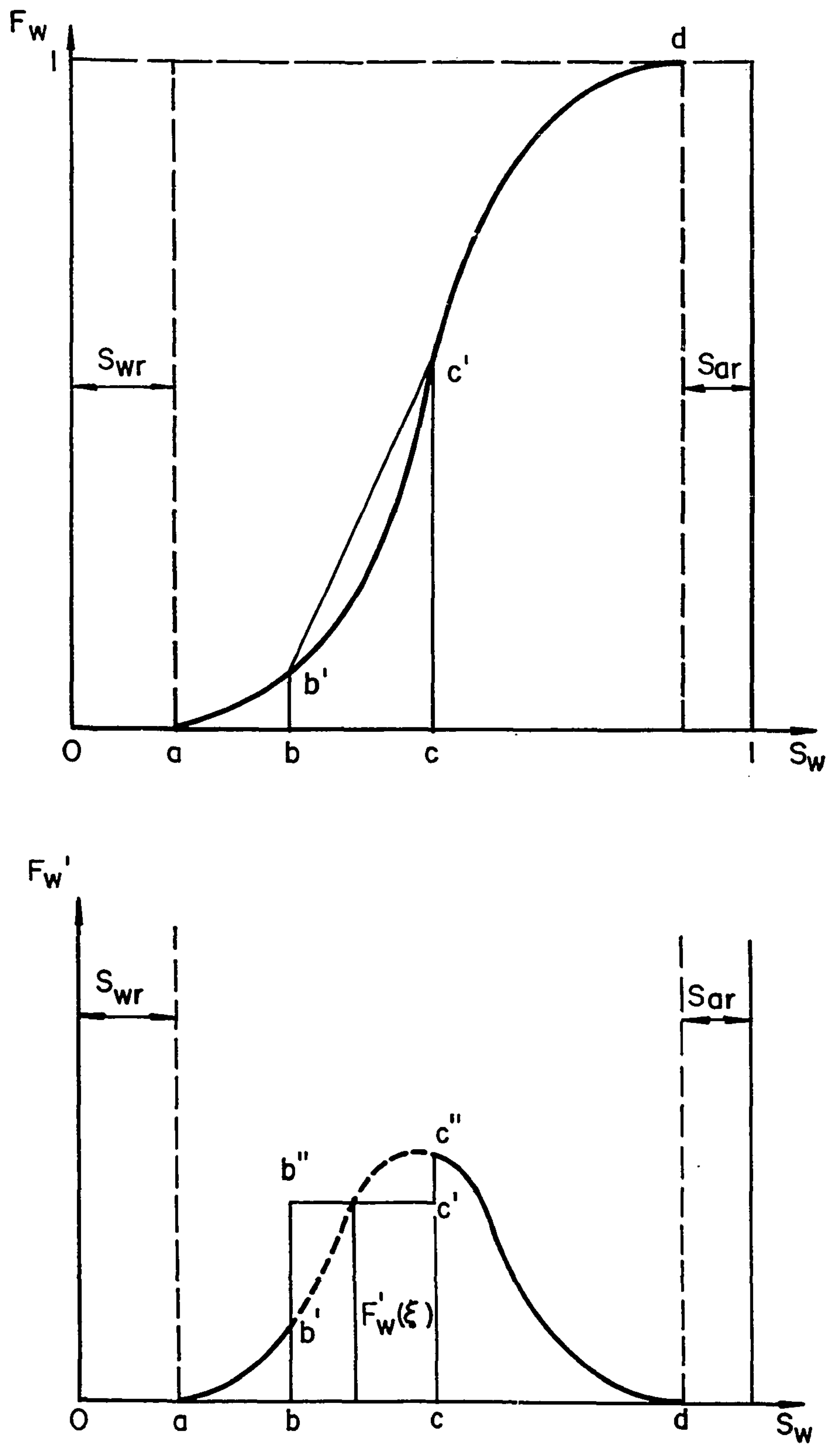

Figure 31 F_w and F_w' Curves with an Arbitrary Secant Construction b' – c'

According to the mean value theorem for integrals (33), there is some value $F'_w(\xi)$ for which

$$\int_b^c F'_{w(S_w)} dS_w = F'_w(\xi) \ (c-b)$$

that is, a material balance is attained. What must $F'_w(\xi)$ be in order to satisfy this relationship? Substituting $\frac{dF_w}{dS_w}$ for $F'_w(S_w)$ in the above equation and rearranging gives

$$F'_w(\xi) = \frac{\int_b^c \frac{dF_w}{dS_w} dS_w}{c-b} = \frac{F_w(c) - F_w(b)}{c - b}$$

Now from the F_w curve, the slope of the secant construction, and hence $F'_w(\xi)$, is

$$\frac{F_w(c) - F_w(b)}{c - b}$$

Therefore the secant construction automatically yields a material balance on the F'_w curve. And since the saturation profile is a function of the F'_w curve, a material balance is attained there too.

APPENDIX 2

SOIL DATA

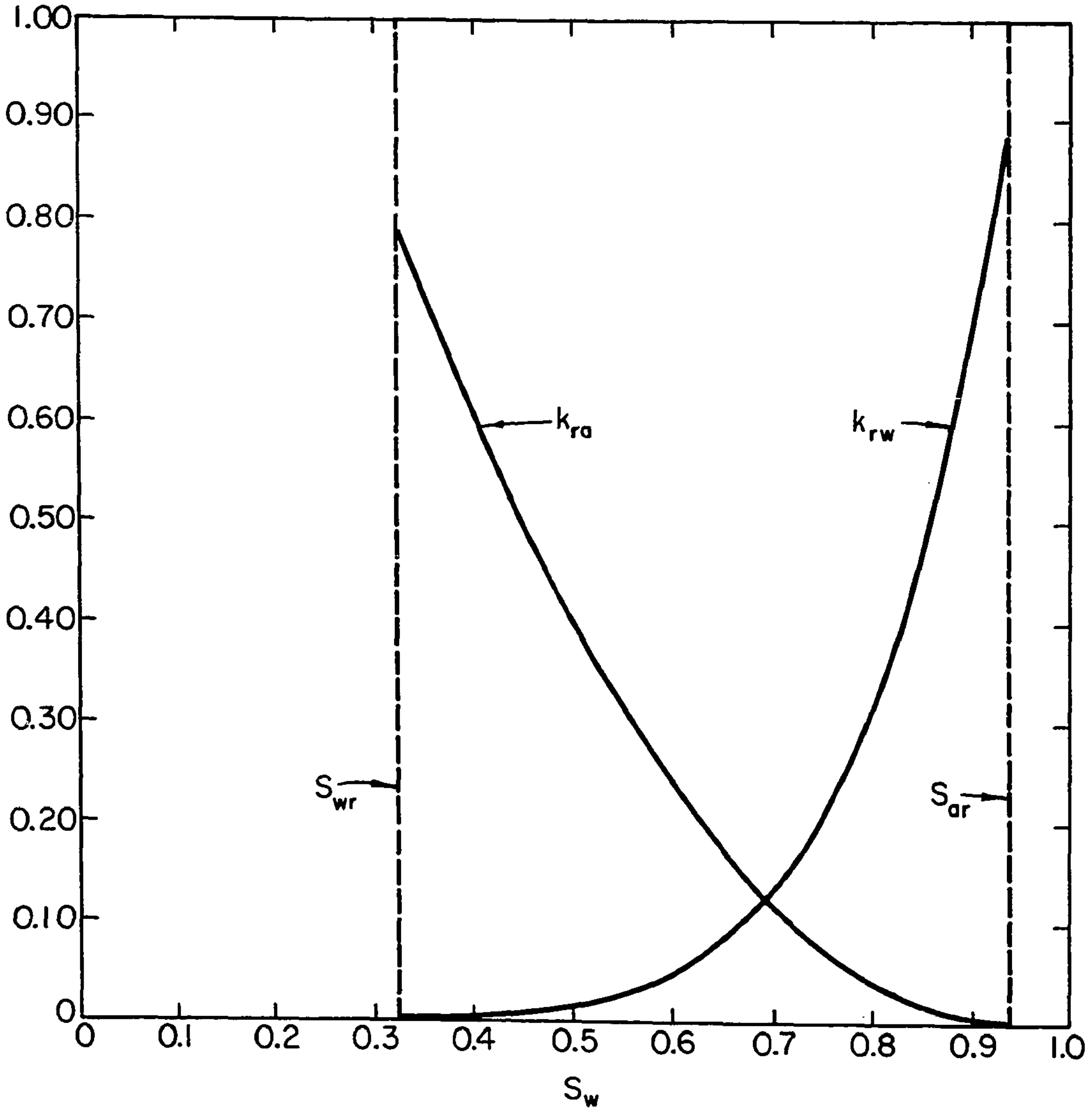

Figure 32 Relative Permeabilities versus Water Saturation

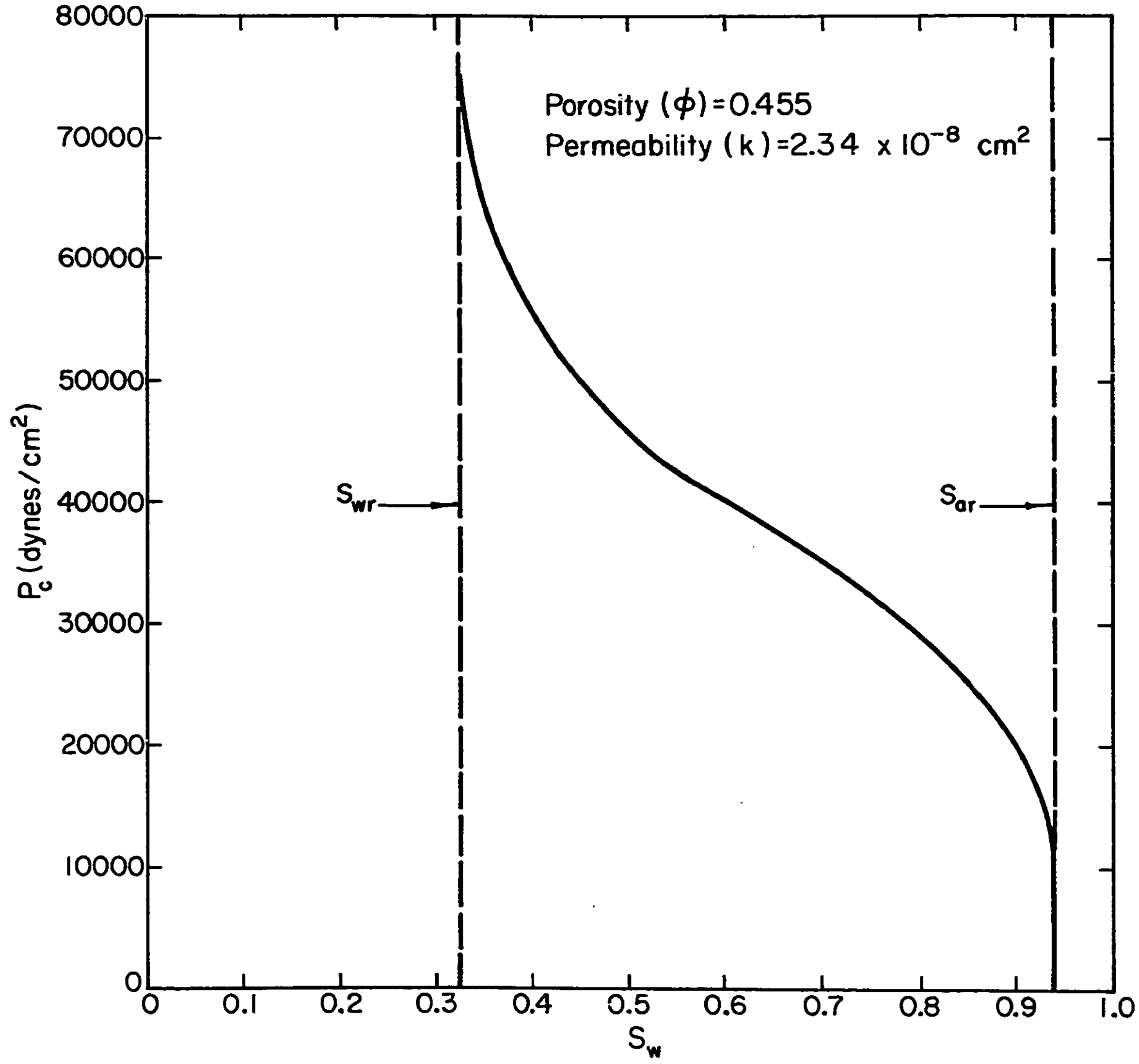

Figure 33 Capillary Pressure versus Water Saturation

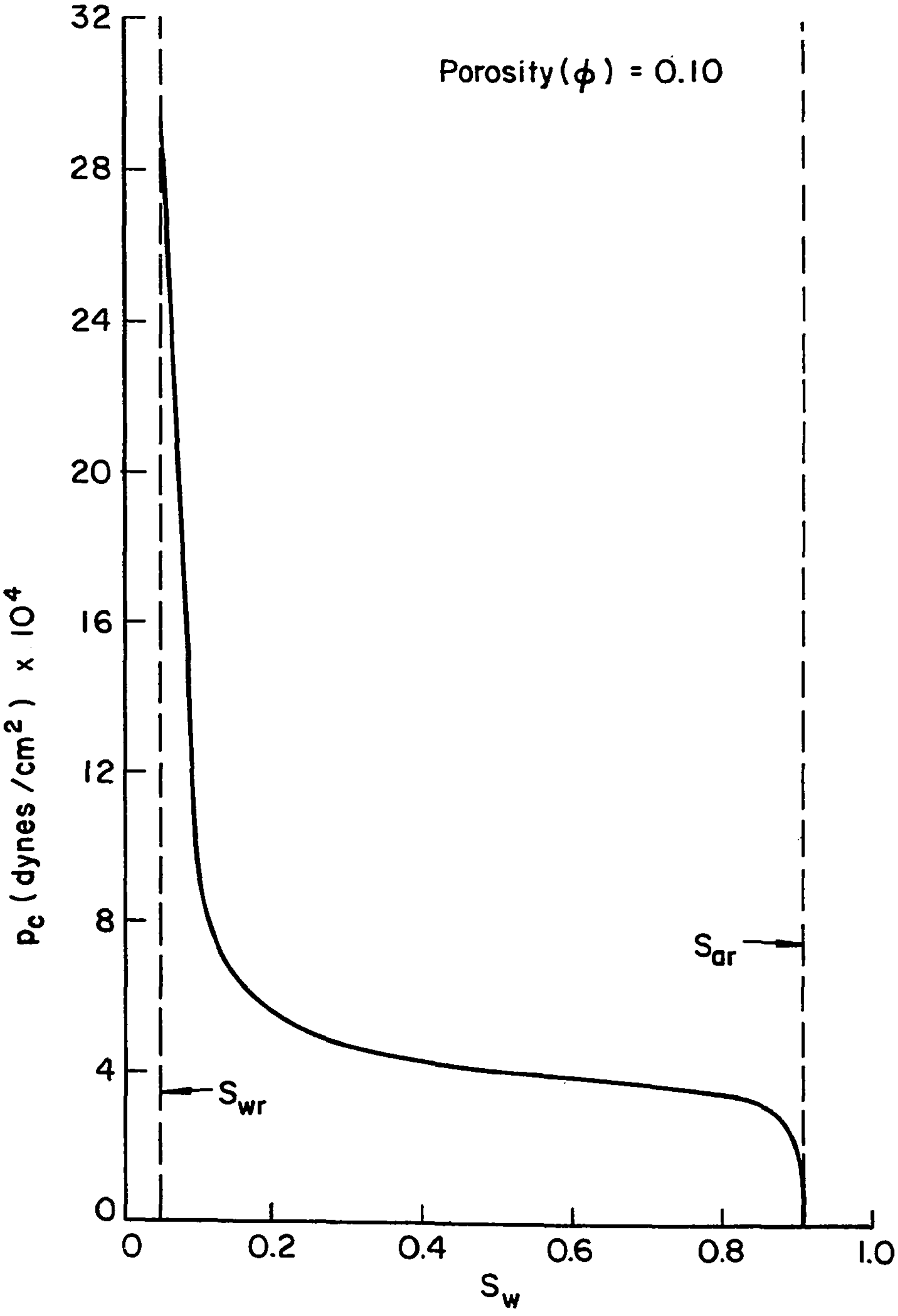

Figure 34 Capillary Pressure versus Water Saturation.

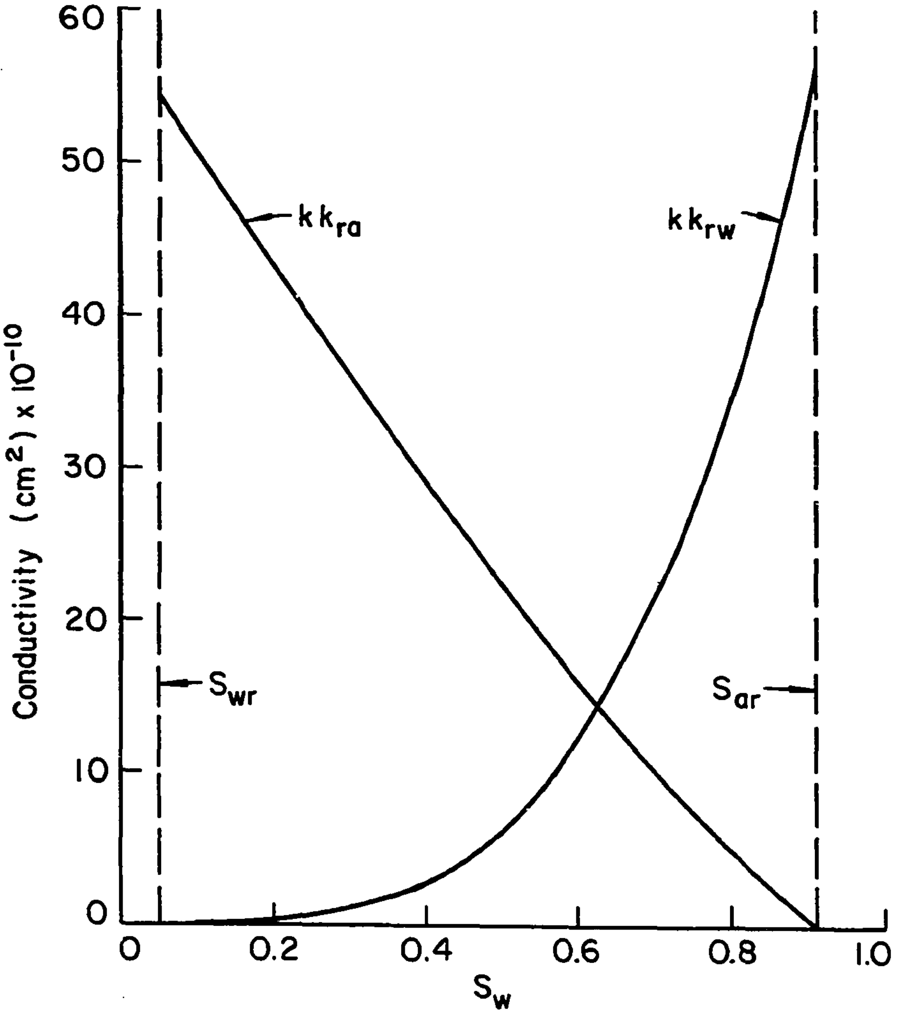

Figure 35 Conductivities of Water and Air.

CED69-70RLB14